Check for updates

JGR Biogeosciences

RESEARCH ARTICLE
10.1029/2021JG006694

Special Section:
Fire in the Earth System

Fire Regions as Environmental Niches: A New Paradigm to Define Potential Fire Regimes in Africa and Australia

M. Zubkova[1], L. Boschetti[2], J. T. Abatzoglou[3], and L. Giglio[1]

[1]Department of Geographical Sciences, University of Maryland, College Park, MD, USA, [2]Department of Forest, Rangeland and Fire Sciences, University of Idaho, Moscow, ID, USA, [3]Management of Complex Systems, University of California, Merced, Merced, CA, USA

Key Points:

- We present a new framework for defining regions (fire regions) with distinct fire-potential based on environmental conditions
- Nine fire regions with significantly different fire characteristics were defined in Africa and eight in Australia
- Different fire patterns were detected within the same biome due to subtle changes in environmental gradient and level of human pressure

Supporting Information:

Supporting Information may be found in the online version of this article.

Correspondence to:

M. Zubkova,
mzubkova@umd.edu

Citation:

Zubkova, M., Boschetti, L., Abatzoglou, J. T., & Giglio, L. (2022). Fire regions as environmental niches: A new paradigm to define potential fire regimes in Africa and Australia. *Journal of Geophysical Research: Biogeosciences*, *127*, e2021JG006694. https://doi.org/10.1029/2021JG006694

Received 28 OCT 2021
Accepted 28 JUN 2022

© 2022. The Authors.
This is an open access article under the terms of the Creative Commons Attribution-NonCommercial-NoDerivs License, which permits use and distribution in any medium, provided the original work is properly cited, the use is non-commercial and no modifications or adaptations are made.

Abstract Despite the widespread use of the "fire regime" concept for describing spatial and temporal patterns and ecosystem impacts of fire, this concept lacks an unambiguous, quantitative definition. By adopting from the ecological literature the concept of climate niche, that is, the environmental conditions that allow a specie to exist, we propose a new framework where variables that promote fuel accumulation and desiccation were used to define the environmental space at the continental level, later divided into regions ("fire regions") with distinct fire potential. Our proposed approach emphasizes climate controls on fire patterns, distinct from the controls that humans exert on observed fire activity. By applying this framework, we identified nine fire regions in Africa and eight in Australia, distinguishing differences in fire patterns between continents as a result of changes in environmental gradient. Not only did we find that fire size and intensity varied significantly between continents, but biomes at a continental level were also found to be heterogeneous in terms of fire frequency, size, and intensity. For example, within African tropical savannas, the total annual rainfall and tree cover change drastically North and South of the equator, resulting in fire regions with significantly different fire characteristics. Meanwhile, in Australia, a strong gradient of annual temperature and precipitation seasonality was observed within tropical savannas and xeric shrublands, which was recognized by dividing those biomes into five regions with statistically different fire activity. Additionally, human presence led to some heterogeneity of fire patterns within delineated fire regions that also varied across biomes.

Plain Language Summary Fire is a natural component of most ecosystems that affects vegetation, soil, water, and the atmosphere. However, the ecosystem impacts of fire vary depending on fire characteristics, including fire size, intensity, and frequency. Here, we proposed a new approach for mapping "fire regions" with distinct patterns of fire activity based on environmental characteristics that promote or limit fuel accumulation and desiccation. We applied this method in Africa and Australia, the two most fire-prone continents, to highlight similarities and distinguish differences in fire activity across continents. The latter were explained by differences in the gradients of those environmental characteristics. As a result, we identified nine fire regions in Africa and eight in Australia that were characterized by biophysical attributes (e.g., climate and vegetation cover) and fire patterns. Significantly, our approach identified regions with distinct fire attributes within individual biomes (most notably within tropical savannas and xeric shrublands) due to differences in environmental controls of fire activity. Our delineated fire regions can be used as a scale unit for fire-statistics calculation and to analyze current fluctuation in fire activity within areas with somewhat homogeneous environmental conditions as a result of changes in human impact to improve our understanding of complex fire-climate-human relationships.

1. Introduction

"Fire regime" is a widely used concept in fire ecology. It originated in the late 19th century, primarily in the French scientific literature on fire practices in Africa. The "fire regime" concept gained widespread use in disturbance ecology since the 1960s and refers to a complementary collection of fire-related parameters that are typically defined differently by ecologists, firefighters, and fire managers (Krebs et al., 2010). The definition of fire regime as "a particular combination of fire characteristics such as fire frequency, size, intensity, severity, seasonality, and fire type" (Gill, 1975) is commonly referenced in works that use global fire satellite products (e.g., Archibald et al., 2013; Chen et al., 2017; Chuvieco et al., 2008; Le Page et al., 2008). Maps of fire regimes are essential for estimating the departure from historical conditions, understanding what drives the geographical distribution of fire regimes, evaluating process-based fire models (Murphy et al., 2011), and for quantifying the

21698961, 2022, 8, Downloaded from https://agupubs.onlinelibrary.wiley.com/doi/10.1029/2021JG006694 by University Of Maryland, Wiley Online Library on [27/09/2023]. See the Terms and Conditions (https://onlinelibrary.wiley.com/terms-and-conditions) on Wiley Online Library for rules of use; OA articles are governed by the applicable Creative Commons License

consequences of fire on biodiversity, ecosystem services, and human society (Aldersley et al., 2011; Lavorel et al., 2007). However, despite an abundance of published studies and the importance of fire-regime maps, an unambiguous, quantitative definition of fire regime does not exist. Controversy remains as to which fire characteristics should be included and how those characteristics should be defined. As a result, maps produced using different definitions of fire regimes are incompatible, precluding consistent quantification of changes in fire activity through time.

A common approach for delineating fire regimes is using several fire metrics in an empirical, data-driven framework (e.g., Archibald et al., 2013; Conedera et al., 2018; Faivre et al., 2011; Le Page et al., 2008). In recent decades, virtually all databases of fire extent and fire characteristics rely on satellite data. Multi-decadal higher resolution (30–250 m) databases are available for North America (e.g., MTBS (Picotte et al., 2020), ABoVE (Loboda et al., 2017)), Australia (e.g., NAFI (NAFI, 2022)), and part of Europe (e.g., EFFIS (San-Miguel-Ayanz et al., 2012)), whereas coarse resolution (500 m) remotely sensed imagery is, for most of the globe, the only available data source that provides coherent multi-temporal fire spatial information since the year 2000 (Benali et al., 2017). The use of global satellite products plays a key role in characterizing fire regimes from the local to the global scale by allowing the systematic computation of fire-related summary metrics such as fire extent, inter-annual variability, seasonality, and intensity (Chen et al., 2017). The choice of fire metrics is constrained to which variables can be quantified at the chosen scale from the selected source of fire data. Fire regime studies typically delineate fire regimes geographically by identifying spatial clusters by way of principal component analysis (PCA, Jiménez-Ruano et al., 2017; Whitman et al., 2015), clustering (e.g., hierarchical (Conedera et al., 2018), k-means (Chen et al., 2017)) or a combination of both (Archibald et al., 2013; Le Page et al., 2008).

While the above-mentioned approach is appealing due to its simplicity, it does not take into consideration the underlying biophysical processes that regulate fire activity, and it is inherently dependent on a number of implicit assumptions. The resulting "fire regime" classification is sensitive to the choice of fire metrics taken into consideration, the mathematical formulation of the metrics, and the spatial scale at which the metrics are computed. Delineating fire regimes based solely on a small number of fire metrics can result in attributing the same fire-regime label to regions where the set of considered fire metrics happens to assume similar values, but the environmental conditions and the ecological implications of fires are very different. Additionally, studies that classify fire regimes from remotely sensed data are fundamentally constrained by the length of the available data archive, which go back at most to 2000 for consistent, well-calibrated global satellite data (Mouillot et al., 2014). Together these issues can lead to a misinterpretation of the processes that drive current fire activity, as well as a misunderstanding of how fire activity might change in the future.

Because of the inherent ambiguity of the concept of fire regime, we propose in this study a new analysis framework based on *fire regions*, drawing from the concept of *climate niche*. This concept is commonly employed in the ecological literature and broadly defined as "the states of the environment which would permit a species to exist" (Hutchinson, 1957). More specifically, in terrestrial ecology, climate niches are defined in terms of geographic and climatic factors that define the habitat of a species (Bonetti & Wiens, 2014; Holt, 2009). We thus define "fire regions" as areas that are homogeneous in terms of environmental conditions that promote fuel accumulation and desiccation, adopting a conceptual model that links specific climate metrics to the key drivers of fire proposed by Bradstock (2010).

The proposed framework was applied in Africa and Australia, the two fire-prone continents responsible for over 75% of the global burned area (Giglio et al., 2018). Tropical savannas are the dominant biome affected by fire on both continents, followed by Xeric shrublands and Mediterranean forest and woodlands (Giglio et al., 2018; Melchiorre & Boschetti, 2018; van der Werf et al., 2017). Similarly, a global study by Archibald et al. (2013) that mapped fire regimes on both continents found that Africa and Australia shared the same fire regimes except for the parts of tropical savannas in Africa that experienced fires smaller in size and with lower intensity, which was primarily attributed to differences in anthropogenic pressure. However, studies by Hantson et al. (2017) and Lehmann et al. (2014) reported dissimilarities in the overall relationships between fire-regime metrics, moisture, and vegetation cover, with the implication that savannas in these two continents might respond differently to future climatic changes.

This study aims to define continental-scale maps of major regions with similar environmental conditions that drive fire activity in Africa and Australia. The hypothesis is that the fire regions delineated solely from environmental

drivers would have distinct values of the fire activity metrics, whereas variations of fire activity within a region would be an indicator of anthropogenic pressure. To this end, we first selected the most important drivers of fire activity in each continent and then used these drivers to define the multi-dimensional environmental space, which was subsequently clustered into distinct fire regions.

Fire-regime metrics (fire frequency, intensity, and size) were utilized to verify the hypothesis that the set of key environmental drivers of fire activity can provide sufficient information to separate regions with different fire characteristics. Finally, we located areas with various degrees of human pressure and explored the gradient of anthropogenic influences on fire activity across the environmental space. We intend that aggregated fire regions can be used as a scale unit for computing fire statistics and assessing current and future trends as a more ecologically meaningful alternative to current fire-regime maps.

2. Data

2.1. Potential Environmental Drivers of Fire Activity

Our proposed approach for defining fire regions is based on the conceptual model of key drivers of pyrogeography proposed by Bradstock (2010), where fire activity is restricted by four "switches": biomass, availability to burn, fire spread, and ignition. Based on previous studies, we identified 12 environmental variables that potentially influence Bradstock's "switches" on a broad scale, including total precipitation, temperature, their intra- and inter-annual variability, water deficit, evapotranspiration, vegetation type, and biomass (Table 1). All variables were calculated/extracted within individual grid cells of a global 0.5° analysis grid, using the same temporal interval (March 2002–February 2019) used to generate the fire activity metrics (Section 2.3). The March-February optimal fire year definition (Boschetti & Roy, 2008) was used instead of the January-December calendar year to avoid artifacts in the time series of annual fire metrics due to the timing of the fire season in Northern Hemisphere Africa (November-February), which would be split between calendar years. Because several of these variables are highly correlated, we retained only six based on the selection procedure described in Section 3.1. For brevity, only these six are described in detail here (Figure S1 in Supporting Information S1):

- *Mean annual temperature* (*Temp*, °C) was defined as the annual average over 17 years. *Temp* was calculated from the Famine Early Warning Systems Network Land Data Assimilation System (FLDAS, McNally et al., 2017) that used outputs from Modern-Era Retrospective Analysis for Research and Applications (MERRA-2, Rienecker et al., 2011) and Climate Hazards Group InfraRed Precipitation with Station data (CHIRPS, Funk et al., 2015). This data set is available as monthly means at 0.1° resolution. Many authors consider *Temp* an important driver of global fire activity (Aldersley et al., 2011; Gillett et al., 2004; Krawchuk & Moritz, 2011). Lehmann et al. (2014) depicted the strong relationship between temperature and fire frequency in Africa and Australia due to temperature's ability to induce plant growth, that is, fuel accumulation, and reduce fuel moisture, which creates favorable conditions for fire ignition and propagation (Daniau et al., 2012; Flannigan et al., 2009).
- *Precipitation Interannual Variability* (*P_Var*) is calculated as the interannual coefficient of rainfall variation, that is, the standard deviation of the time series of annual rainfall divided by its mean based on FLDAS data; the annual precipitation totals were computed using the fire year definition. Moisture fluctuation, specifically in semi-arid regions, affects fuel accumulation rates and fuel connectivity, which enables bigger, more intense fires (Bradstock, 2010; Murphy et al., 2013). Consequently, the extent of area burned varies substantially between years with a "wet" dry season and with a "dry" dry season (Mulqueeny et al., 2011). Additionally, in forested regions where high levels of moisture usually prevent fire ignition and propagation, prolonged droughts can create suitable conditions for fire (Cochrane, 2003; van der Werf et al., 2008).
- *Precipitation amplitude* (*P_Amp*, mm) was defined as the difference in average precipitation between the wet and dry seasons following the Saha et al. (2019) approach (see SI for calculation) based on FLDAS data. It is widely accepted that the temporal fluctuation in moisture availability is one of the main drivers of fire activity (Krawchuk et al., 2009; Markham, 1970; Murphy & Bowman, 2007; Staver et al., 2011), and here *P_Amp* was used to characterize the weather conditions that favor desiccation, which is necessary for fire ignition and propagation once sufficient fuel is accumulated.
- *Seasonality index* (*P_SI*) characterizes the extent to which a yearly precipitation cycle can be partitioned into well-defined wet and dry seasons (Saha et al., 2019, SI), thus complementing *P_Amp* in describing the intra-annual precipitation variability. *P_SI* assumes values close to 1 if a particular region has two distinct

21698961, 2022, 8, Downloaded from https://agupubs.onlinelibrary.wiley.com/doi/10.1029/2021JG006694 by University Of Maryland, Wiley Online Library on [27/09/2023]. See the Terms and Conditions (https://onlinelibrary.wiley.com/terms-and-conditions) on Wiley Online Library for rules of use; OA articles are governed by the applicable Creative Commons License

Table 1
Summary of the Potential Drivers of Fire Activity Considered in the Analysis

Variable name	Abbreviation and units	Description	Source
Climate			
Mean annual precipitation	P, mm	Average of the time series of annual total precipitation	FLDAS (the Famine Early Warning Systems Network Land Data Assimilation System) (McNally et al., 2017)
Precipitation amplitude (*)	P_Amp, mm	Difference in average precipitation between wet and dry seasons. Calculated using Saha et al. (2019) approach	FLDAS (McNally et al., 2017)
Seasonality index (*)	P_SI, unitless	Measure of precipitation seasonality (Saha et al., 2019)	FLDAS (McNally et al., 2017)
Precipitation interannual variability (*)	P_Var, unitless	Coefficient of variation of the annual total precipitation (the standard deviation of the time series divided by the mean)	FLDAS (McNally et al., 2017)
Mean annual temperature (*)	Temp, °C	Annual temperature average over 17 years (Mar 2002–February 2019)	FLDAS (McNally et al., 2017)
Temperature amplitude	T_Amp, °C	Difference in average temperature between cold and hot seasons (Saha et al., 2019)	FLDAS (McNally et al., 2017)
Mean temperature of the warmest month	T_Max, °C	Monthly temperature averaged over the month with the highest temperature	FLDAS (McNally et al., 2017)
Actual evapotranspiration (*)	AET, mm	Calculated using a Thornthwaite-Mather climatic water-balance model (Willmott et al., 1985)	TerraClimate (Abatzoglou, Williams, et al., 2018)
Potential evapotranspiration	PET, mm	Calculated using Penman-Monteith approach (Allen et al., 1998)	TerraClimate (Abatzoglou, Williams, et al., 2018)
Climatic water deficit	DEF, mm	Defined as the difference between PET and AET	TerraClimate (Abatzoglou, Williams, et al., 2018)
Vegetation			
Tree cover (*)	Tree, %	Percent tree cover	MOD44B Version 6 (https://modis.gsfc.nasa.gov/data/dataprod/mod44.php)
Aboveground biomass	Biomass, Mg C/ha	Aboveground biomass carbon density for 2010	Global Aboveground and Belowground Biomass Carbon Density Maps (https://doi.org/10.3334/ORNLDAAC/1763)

Note. An asterisk indicates the six climate and vegetation variables retained after the initial screening (Section 3.1). All climate variables are calculated from 17 years of data (2002–2019).

precipitation seasons (i.e., one wet and one dry season) and close to 0 otherwise. Prolonged dry seasons in mesic savannas desiccate fuels and contribute to high burning rates (Leys et al., 2018; van der Werf et al., 2008). In wet environments, the absence of a highly defined dry season promotes tree cover growth, where an increase in the duration of the dry season reduces tree cover and increases the chances of fire occurrence (Staver et al., 2011).

- *Percent tree cover* (*Tree*, %) calculated from the Collection 6 MODIS MOD44B Global Vegetation Continuous Fields product (DiMiceli et al., 2017). Fire behavior varies strongly across the savanna-forest boundaries (Hoffmann et al., 2012; Zubkova et al., 2019). The type of vegetation influences the likelihood of fire (Lehmann et al., 2011), and Archibald et al. (2009) identified tree cover as one of the main drivers of the amount of burned area in Southern Africa due to its negative impact on grass biomass and, therefore, the fire spread.
- *Mean annual actual evapotranspiration* (*AET*, mm) was acquired from TerraClimate (Abatzoglou, Dobrowski, et al., 2018) based on a one-dimensional water-balance model (WBM, Willmott et al., 1985). Fuel productivity and dryness are a function of climatic water balance (Boer et al., 2016). At annual timescales, *AET* can be considered a reliable predictor of continental patterns of primary productivity (Rosenzweig, 1968; Yang et al., 2013).

21698961, 2022, 8, Downloaded from https://agupubs.onlinelibrary.wiley.com/doi/10.1029/2021JG006694 by University Of Maryland, Wiley Online Library on [27/09/2023]. See the Terms and Conditions (https://onlinelibrary.wiley.com/terms-and-conditions) on Wiley Online Library for rules of use; OA articles are governed by the applicable Creative Commons License

21698961, 2022, 8, Downloaded from https://agupubs.onlinelibrary.wiley.com/doi/10.1029/2021JG006694 by University Of Maryland, Wiley Online Library on [27/09/2023]. See the Terms and Conditions (https://onlinelibrary.wiley.com/terms-and-conditions) on Wiley Online Library for rules of use; OA articles are governed by the applicable Creative Commons License

2.2. Anthropogenic Pressure

Human presence profoundly alters fire activity in any ecosystem, with multiple direct and indirect effects on the number, extent, and intensity of fire events. Humans increase the number of ignitions but also lead to fire suppression, as well as alterations to vegetation composition, biomass availability, and landscape connectivity, that is, the human population density was found to impact three of the four "switches" of the Bradstock (2010) model (Aldersley et al., 2011; Archibald, 2016; Archibald et al., 2009; Kahiu & Hanan, 2018). In addition to population density, we considered the proportion of natural vegetation and the livestock density as variables reflecting different aspects of anthropogenic pressure relevant to fire (Archibald, 2016; Archibald et al., 2009, 2013; Guyette et al., 2002; Sanderson et al., 2002; Syphard et al., 2017). The proportion of natural vegetation is a proxy for fuel connectivity and landscape fragmentation, a decrease of which negatively impacts fire spread, whereas grazers remove biomass and compete with fire for fuel, thus having a negative effect on the area burned and on fire intensity.

The three gridded anthropogenic pressure variables are defined as follows:

- *Population density* (*Pop*, units: people/km^2): the population density was calculated from the Gridded Population of the World (GPWv4) 2010 data set (CIESIN, 2016)
- *Proportion of natural vegetation* (*Nat_veg*, unitless [0–1]): defined as the proportion of all land cover types excluding cropland, urban, and unburnable surfaces in a grid cell based on the Climate Change Initiative Global Land Cover (CCI LC) product (2015, CCI-LC-PUGV2, 2017).
- *Livestock density* (*LS*, units: TLU/km^2): defined in equivalent Tropical Livestock Units (TLU), applying the conversion factors for cattle (0.70), sheep and goats (0.10) proposed by Pica-Ciamarra et al. (2007) using Gridded Livestock of the World (GLW3) 2010 (Gilbert et al., 2018).

The anthropogenic pressure variables were used in the evaluation of fire regions (Section 3.3).

2.3. Fire Activity Metrics

Three metrics of fire activity, commonly used in published local to global fire studies, were calculated on 0.5° grid cells from the available MODIS fire products (Figure S3 in Supporting Information S1):

- *Percent mean annual burned area* (*BA*, %), calculated as the annual average over 17 years from the Collection 6 MODIS global burned area product (MDC64A1). MCD64A1 is a monthly gridded product, mapping the burned area location and approximate day of burning at 500 m resolution (Giglio et al., 2009).
- *Maximum fire size* (*FSize*, km^2) was defined as the 95th percentile of the fire size distribution. The fire size distribution was calculated by extracting individual fire events from the MCD64A1 product through a novel flood-fill algorithm that uses the spatial and temporal burned area information and the uncertainty layer to define a locally adjusted temporal threshold (Humber, 2019). Due to the reduced accuracy of small fire detection (Boschetti et al., 2019), fires covering less than five cells (<1.07 km^2) on the 500-m MODIS sinusoidal grid were excluded from the analysis.
- *Maximum fire radiative power* as a proxy for *fire intensity* (*FRP*, MW) was defined as the 95th percentile of the *FRP* distribution extracted from the Collection 6 MODIS MCD14ML fire location product (Giglio et al., 2016). MCD14ML is a summary product reporting all the active fires detected as actively burning at the satellite overpass under relatively cloud-free conditions with a nominal spatial resolution of 1 km. *FRP* was calculated by taking into account the variable pixel size in the across-track direction (Giglio, 2013). Only fire points with "nominal" or "high" confidence, detected within natural land, were included in the analysis.

As with the environmental variables, fire metrics were computed using the fire year definition utilizing data from March 2002 to February 2019. The first two years of MODIS data (2000–2001) were not used due to sensor calibration problems and acquisition outages (Giglio et al., 2016).

The fire activity metrics were used to inform the selection of the environmental variables (Section 3.1) and evaluate the resulting fire regions (Section 3.3).

21698961, 2022, 8, Downloaded from https://agupubs.onlinelibrary.wiley.com/doi/10.1029/2021JG006694 by University Of Maryland, Wiley Online Library on [27/09/2023]. See the Terms and Conditions (https://onlinelibrary.wiley.com/terms-and-conditions) on Wiley Online Library for rules of use; OA articles are governed by the applicable Creative Commons License

2.4. Burnable Land Mask

To avoid assigning fire regions to areas that do not experience fire activity due to the lack of vegetation, we created a burnable land mask. First, the proportion of burnable vegetation (i.e., all land cover types except urban, bare soil, and water from the CCI LC product) was calculated within each 0.5° cell. The relationship between *BA* and the proportion of vegetation was subsequently analyzed within each continent. We found that *BA* increases with the proportion of burnable land following an exponential distribution, with nominal fire activity in areas of low vegetation cover (<0.74 in Africa, <0.88 in Australia; Figure S4 in Supporting Information S1). These thresholds were calculated using the Unit Invariant Knee point as an objective estimator for the elbow criterion (Christopoulos, 2016). All grid cells with the proportion of burnable vegetation below estimated thresholds were excluded from further analysis.

3. Methods

The fire regions were mapped by means of a statistical analysis based on principal component (PCA) and clustering of gridded environmental driver variables, following established approaches for identifying regions with similar spatiotemporal characteristics. PCA is used to identify patterns in the data which might not be obvious when a data set contains a large number of variables that are not statistically independent (Le Page et al., 2008), which is common in ecological and climatological studies (e.g., Abatzoglou et al., 2009; Archibald et al., 2013; Faivre et al., 2011; Whitman et al., 2015). While PCA can handle some degree of multicollinearity, previous research has suggested setting aside highly correlated variables to reduce the bias of PCA results (Jiang & Eskridge, 2000). Including the nearly-redundant variables can cause the PCA to overemphasize their contribution. For this reason, the first processing step (Figure 1, green dotted box) was the selection of the input variables, removing those with high collinearity (Section 3.1). The fire regions were then identified through hierarchical clustering of the principal components (PC) of the inputs, a method commonly used in fire studies since (a) it does not require the prior definition of the number of target clusters and (b) it is suitable for the definition of biogeographic regions which are hierarchically arranged (Conedera et al., 2018; Faivre et al., 2011; Le Page et al., 2008). The clusters were aggregated using the WWF Terrestrial Ecoregions of the World (Olson et al., 2001), resulting in the final fire region map (Figure 1 red dotted box, Section 3.2). Finally, the fire region map was evaluated by analyzing the difference in fire characteristics across regions and the impact of anthropogenic factors within regions (Figure 1 blue dotted box, Section 3.3).

3.1. Selection of the Environmental Drivers

Collinearity among variables was assessed by calculating pair-wise Pearson's correlation coefficients separately for Africa (Figure S5 in Supporting Information S1) and Australia (Figure S6 in Supporting Information S1). Correlation coefficients higher than 0.65 or lower than −0.65 indicated high collinearity, adopting the threshold value frequently utilized in the literature (Monjarás-Vega et al., 2020; Oliveira et al., 2014). Uncorrelated variables (*P_Amp* and *P_SI* in Africa, *P_Var* and *P_SI* in Australia) were directly included in the PCA, while the rest had to undergo additional exploratory analysis based on bivariate generalized additive models (GAMs, Wood & Wood, 2017). GAMs were generated to investigate the relationship between each of the remaining highly correlated variables and the three fire metrics in Africa (Figure S7 in Supporting Information S1) and Australia (Figure S8 in Supporting Information S1). Among sets of highly correlated variables, the one which is a better predictor for a majority of the fire metrics (i.e., higher explained deviance, reported in the upper right corner of each plot in Figures S7 and S8 in Supporting Information S1) was selected as follows.

In Africa:

- *Tree* was selected from the highly correlated set *{Tree*, *Biomass*, *P}* because it was a better predictor of *BA* and *FRP*.
- *AET* was selected from *{PET*, *DEF*, *AET}* because it was a better predictor for *BA* and *FRP*.
- *Temp* was selected from *{Temp*, *T_Max}* because it was a better predictor for *FSize*, and substantially equivalent for *BA* and *FRP*.
- *P_Var* was included because it correlates highly only with *P*, which was excluded as detailed above.

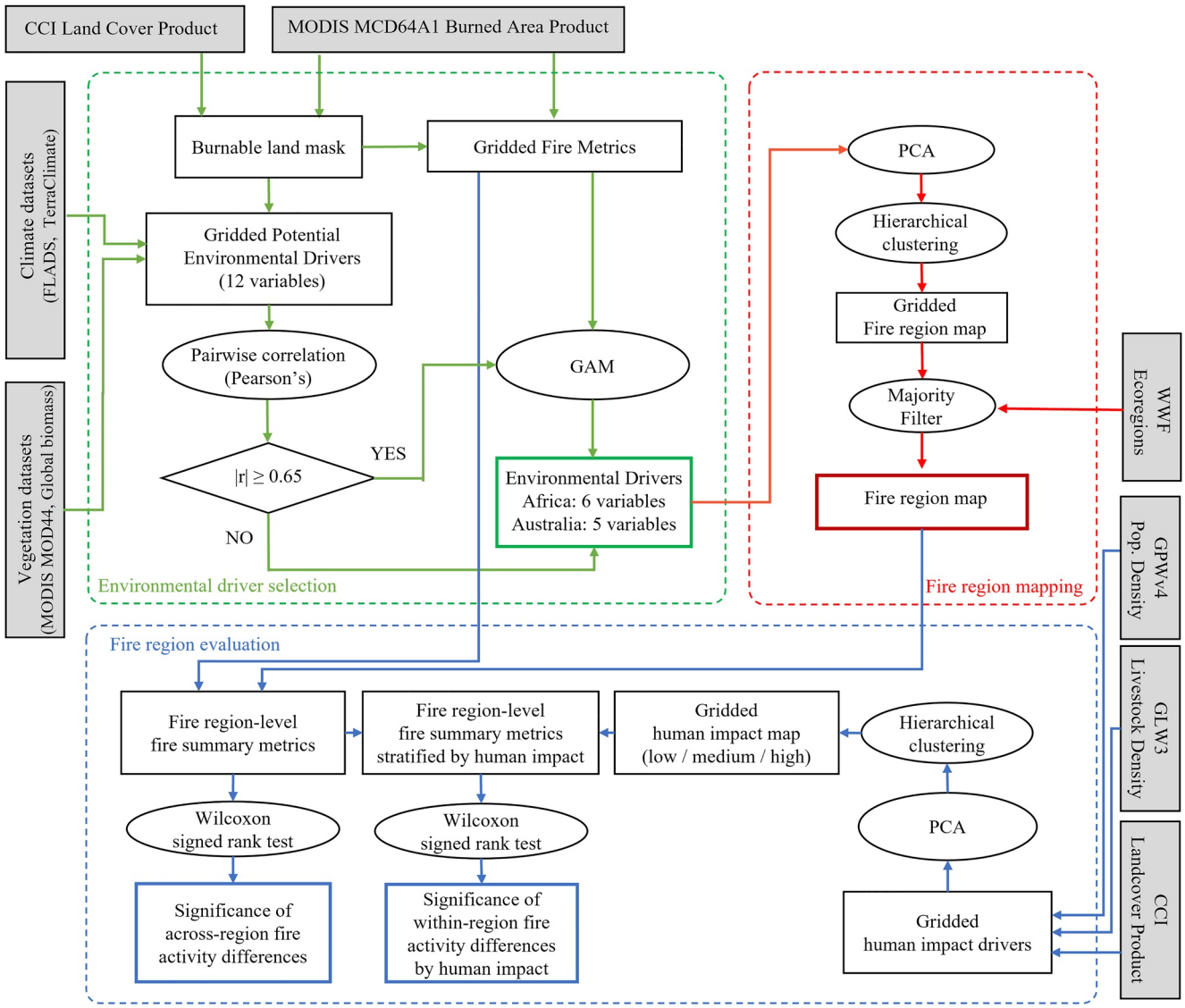

Figure 1. Flowchart illustrating the main processing steps; following standard conventions, rectangles are used for datasets, ovals for processes and diamonds for Boolean operators. The dotted rectangles encompass the three main processing steps described in details in Sections 3.1 through 3.3.

In Australia:

- *P_Amp* was selected from *{P_Amp*, *P*, *AET*, *PET*, *DEF*, *T_Amp}* because it was a better predictor of *BA* and *FSize*.
- Temp was selected from *{Temp*, *T_Max}* because it was a better predictor of all three fire metrics.
- Tree was selected from *{Tree*, *Biomass}* because it was a better predictor of all three fire metrics.

The two steps of the exploratory analysis resulted in the selection of six environmental drivers in Africa (*Temp*, *P_Amp*, *P_SI*, *P_Var*, *Tree*, *AET*) and five in Australia (*Temp*, *P_Amp*, *P_SI*, *P_Var*, *Tree*).

3.2. Fire Region Mapping

PCA and clustering were performed separately for Africa and Australia since these two continents vary in terms of vegetation cover and level of anthropogenic pressure, which can alter the climate-fire relationships among continents (Archibald et al., 2010; Lehmann et al., 2014; Stevens et al., 2017). To ensure that all variables have equal weights, all data were normalized by rescaling the values between 0 and 1 and centered (Mardia et al., 1979).

21698961, 2022, 8, Downloaded from https://agupubs.onlinelibrary.wiley.com/doi/10.1029/2021JG006694 by University Of Maryland, Wiley Online Library on [27/09/2023]. See the Terms and Conditions (https://onlinelibrary.wiley.com/terms-and-conditions) on Wiley Online Library for rules of use; OA articles are governed by the applicable Creative Commons License

21698961, 2022, 8, Downloaded from https://agupubs.onlinelibrary.wiley.com/doi/10.1029/2021JG006694 by University Of Maryland, Wiley Online Library on [27/09/2023]. See the Terms and Conditions (https://onlinelibrary.wiley.com/terms-and-conditions) on Wiley Online Library for rules of use; OA articles are governed by the applicable Creative Commons License

Clustering was based on a Euclidean distance matrix computed using all PCs with eigenvalue >1 (Girden, 2010). Grid cells were incrementally merged into clusters using Ward's linkage method (Ward, 1963), according to which the distance between two clusters is equivalent to an increase of the sum of squares when they are being merged. The number of clusters was determined by inspecting the dendrograms. Following the recommendations by Wilks (2005), moving from the bottom to the top of the dendrogram, at each step, the distance between merged clusters is computed as defined above, and the merging process is stopped one step before the distance between merged clusters jumps markedly (i.e., before a discontinuity in the derivative of the distance). The selection of the number of clusters was a compromise between the highest separation between clusters based on the dendrograms and selecting enough clusters to represent the full range of environmental gradients at the continental level.

Due to the continuous nature of environmental variables, clustering of grid cells can lead to a noisy output map, making it difficult to interpret or use for ecological applications. For that reason, once each 0.5° grid cell was assigned to a cluster, the results were aggregated at the ecoregion scale using a majority overlap criterion. The Olson et al. (2001) ecoregions, defined as large areas of relatively uniform climate and vegetation that are refuge to a specific set of species and ecological communities, were used because of commonalities in vegetation that mediate climate-fire relationships (Abatzoglou, Williams, et al., 2018; Pausas & Fernández-Muñoz, 2012; Zubkova et al., 2019).

3.3. Evaluation of the Fire Regions

To evaluate the separability of the proposed fire regions in terms of fire activity, we compared fire metrics within each region using the Wilcoxon signed-rank test. The Wilcoxon test is a nonparametric test that can be used to test the significance of the differences between the means of two samples (Wilcoxon, 1945). Fire regions were analyzed within each continent and between continents to test if similar environmental conditions lead to similar fire activity in different geographical regions.

Additionally, within each fire region, we tested if different levels of anthropogenic pressure led to significant variation in fire activity, thus separating environmental drivers of fire from human influences to evaluate human drivers within different climate niches. We ran the PCA and clustering procedure on the three anthropogenic pressure variables for each continent, resulting in continental maps of clusters homogeneous in terms of anthropogenic pressure. We then stratified each region by the level of anthropogenic pressure to verify whether it significantly affected the fire metrics.

4. Results

4.1. Fire Regions

The PCA analysis was performed to reduce the dimensionality of the set of environmental drivers; in both continents, only the first three PCs had eigenvalues >1, and were therefore used in the subsequent hierarchical clustering. Like Faivre et al. (2011), we cut the dendrograms into several clusters of increasingly complex biophysical patterns. A simple pattern would lead to 5 clusters in Africa and 4 clusters in Australia, while a more complex pattern included 9 clusters in Africa and 8 in Australia (Figure S9 in Supporting Information S1). Beyond this, the distance between clusters was negligible, meaning similarities between clusters were drastically increasing; therefore, further splitting of the data was not justified.

Figure 2 shows the fire regions as scatterplots in the space of the first three PCs, whereas Figure 3a shows the gridded fire region map at 0.5° resolution, which were subsequently aggregated at the ecoregion scale through the application of a majority filter (Figure 3b).

To allow for unambiguous labeling of the fire regions, each is identified by a three-digit numerical code, where the first digit indicates the realm (1 - Australasian, 3 - Afrotropical), the second digit indicates the label from the first split (simple pattern), which was based on the mean value of the first PC, ranked from high to low, while the third digit is based on the further split (Figure S9 in Supporting Information S1). It follows that regions whose codes have the same first two digits share more similarities than regions with entirely different codes. For example, the environmental space between clusters 321, 322, and 323 is more similar than between clusters 321 and 311. The digit "1" in the numeric code "321" means that cluster 321 had the highest mean value of the first PC compared to clusters 322 and 323 (Figures 2 and 3).

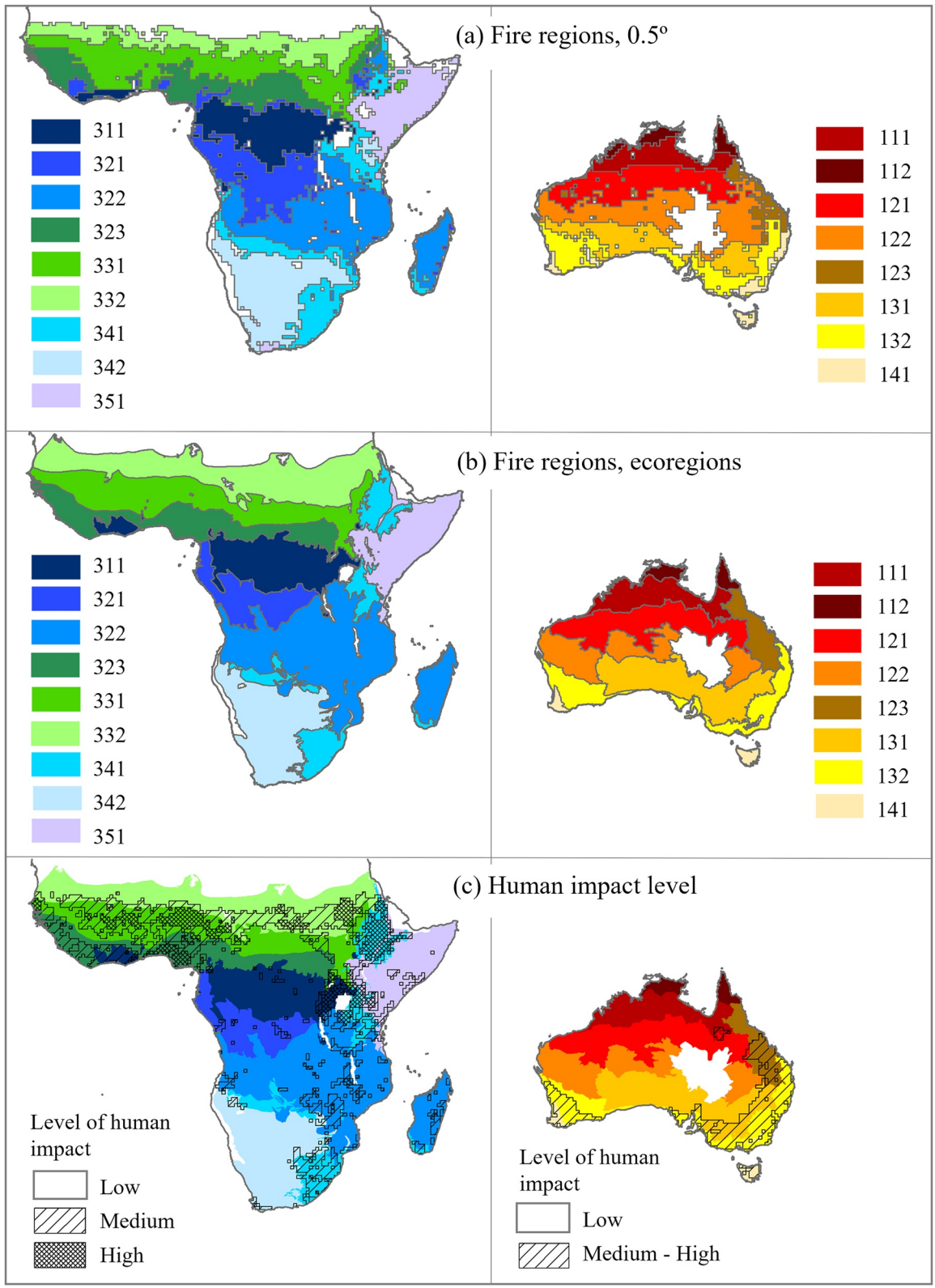

Figure 2. Position of the fire regions within the space of the environmental variables in Africa (left) and Australia (right). Biplots show the ordination of 0.5° cells along the first and second principal components (PC) (top row) and first and third PC (bottom row); cell symbols indicate the fire regions (i.e., the cluster each cell is assigned to).

21698961, 2022, 8, Downloaded from https://agupubs.onlinelibrary.wiley.com/doi/10.1029/2021JG006694 by University Of Maryland, Wiley Online Library on [27/09/2023]. See the Terms and Conditions (https://onlinelibrary.wiley.com/terms-and-conditions) on Wiley Online Library for rules of use; OA articles are governed by the applicable Creative Commons License

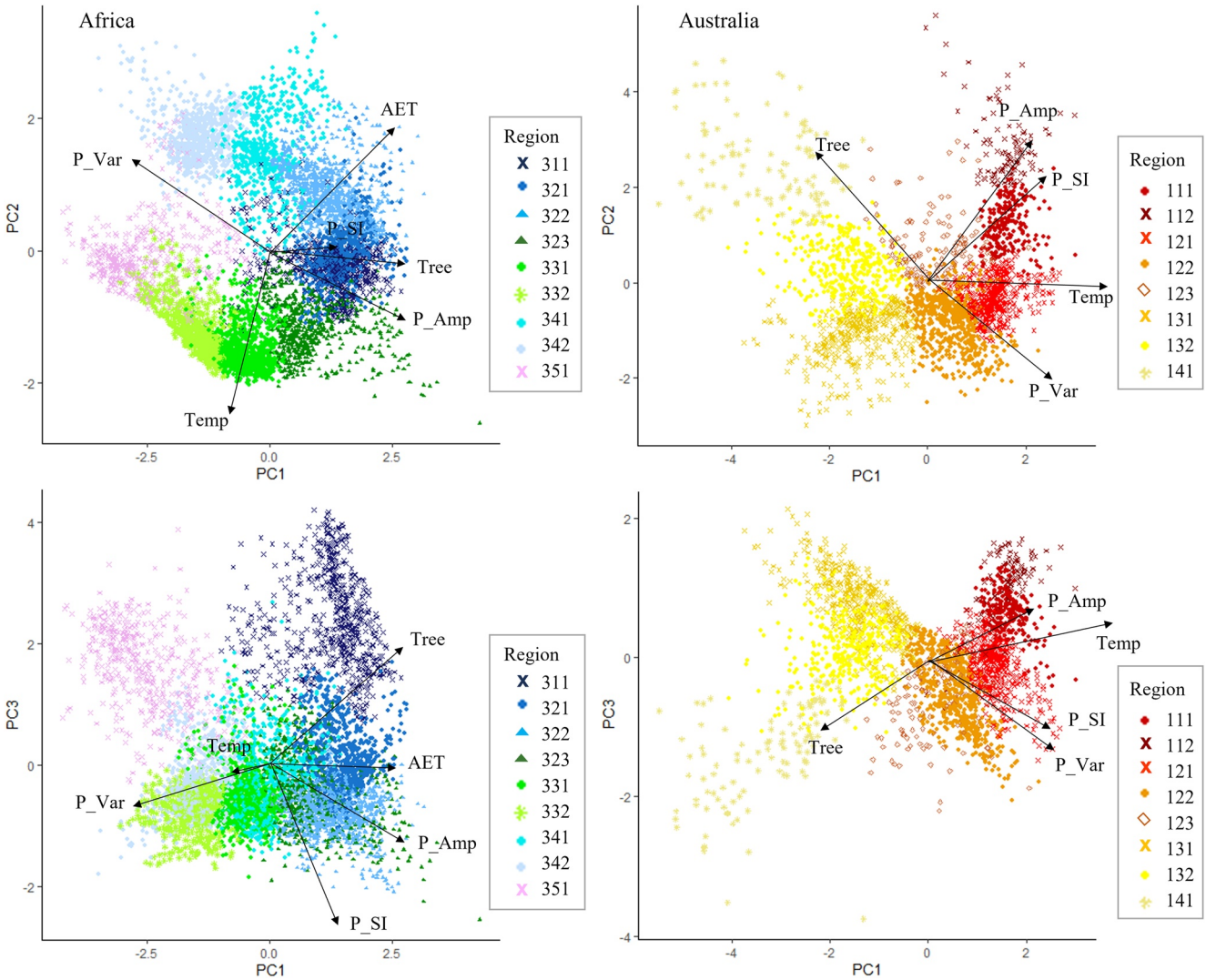

Figure 3. Spatial distribution of major fire regions in Africa and Australia. (a) Gridded fire region map at 0.5° resolution; (b) final fire region map, obtained by aggregating the gridded data at the ecoregions level; (c) human impact level map, (black vectors) overlaid with the fire regions maps. White color represented unburnable surfaces and areas where the vegetation is too sparse to sustain any substantial fire activity.

In both continents, the first two PCs were driven by the *Tree*, *P_Amp*, and *Temp* gradient (Figure 2). In Africa, the primary gradient was related to *P_Var*, *P_Amp*, and *Tree*, splitting the continent into regions with low *P_Var* and high *Tree* (Figure 3, region 311–323, *P_Var* = 0.1 and *Tree* = 32.5% on average) and high *P_Var* and low *Tree* (regions 331–351, *P_Var* = 0.2, *Tree* = 6.6%). The second PC was driven by *Temp* and *AET* that further split high *P_Var* regions into hot, Sahel (region 331–332, *Temp* = 27.8 °C), medium, Horn of Africa (region 351, *Temp* = 25.0 °C), and cold, deserts and xeric shrublands (region 341–342, *Temp* = 20.7 °C), while the third PC was related to *P_SI* that helped to differentiate between tropical forest (region 311, *P_SI* = 0.7) and savannas (regions 321–323, *P_SI* = 0.9). In Australia, *Temp* was a primary gradient that split the continent into hot (region 111–123, *Temp* = 24.2°C) and cold (region 131–141, *Temp* = 17.8°C) regions, where the second PC attributed to *P_Amp* and *Tree* split hot regions further into high *P_Amp*, tropical savannas (region 111–112, *P_Amp* = 192 mm) and low, deserts and xeric shrublands (region 121–123, *P_Amp* = 48 mm) and cold regions into high *Tree*, temperate forest (region 141, *Tree* = 48.4%) and low, Mediterranean forest and temperate grasslands (region 131–132, *Tree* = 18.3%).

21698961, 2022, 8, Downloaded from https://agupubs.onlinelibrary.wiley.com/doi/10.1029/2021JG006694 by University Of Maryland, Wiley Online Library on [27/09/2023]. See the Terms and Conditions (https://onlinelibrary.wiley.com/terms-and-conditions) on Wiley Online Library for rules of use; OA articles are governed by the applicable Creative Commons License

21698961, 2022, 8, Downloaded from https://agupubs.onlinelibrary.wiley.com/doi/10.1029/2021JG006694 by University Of Maryland, Wiley Online Library on [27/09/2023]. See the Terms and Conditions (https://onlinelibrary.wiley.com/terms-and-conditions) on Wiley Online Library for rules of use; OA articles are governed by the applicable Creative Commons License

4.2. Evaluation of the Fire Regions

4.2.1. Across-Region Variations in Fire Activity

The overall relationship between *BA* and the environmental drivers was similar in the two continents: the highest *BA* was detected in regions with strong precipitation seasonality (i.e., *P_Amp*, and *P_SI*), while regions with high *Tree* had the lowest *BA* (Figures 4 and 5). Similarly, the results of the GAMs (Figures S7 and S8 in Supporting Information S1) showed that both rainfall seasonality variables had a positive relationship with *BA*, albeit not for the entire range of the two variables. In particular, *BA* increases with *P_Amp* until it reaches about 200 mm, and with $P\_SI > 0.5$.

In Africa, *BA* initially increases with *Tree* and *P*, reaching a maximum at approximately *Tree* = 20% or *P* = 1,200 mm, and then decreases, confirming the intermediate fire–productivity hypothesis (Pausas & Ribeiro, 2013; van der Werf et al., 2008) and would indicate that in xeric environments *P*—which drives the availability of fuel—is the main fire limiting factor (i.e., water-limited systems). In wetter environments, however, fuel is not a limiting factor, but precipitation seasonality (measured by *P_Amp*), with the presence of distinct wet and dry seasons, is (i.e., energy-limited systems). High *P* and low *P_Amp* create favorable conditions for tree growth, and at *Tree* >60% we observed a drastic reduction of *BA* in Africa (Figure S7 in Supporting Information S1). We note that although *P* was not explicitly used in the fire region clustering due to strong collinearity with *Tree* (Africa) and *P_Amp* (Australia), changes in fire activity as a function of the *P* gradients were reported to acknowledge that—on the physical level—*P* remains one of the key drivers of fire activity in the tropics.

In Australia, the relationship between *BA* and *P* shows a similar pattern but significantly less pronounced, with a much wider spread of the confidence interval at high *P* values (>1500 mm). This pattern reflects the fact that, in Australia, some of the areas with the highest *P* also have high *P_Amp* and consequently experience high fire activity (i.e., Northern Australia). In contrast, other areas have high *P* and low *P_Amp*, and therefore experience low *BA* (i.e., the South East of the continent and Tasmania).

Large fires in both continents were observed within areas with similar environmental conditions. In general, *FSize* tends to increase with *P_SI* and *P_Var* and decreases with *Tree* (Figures 4 and 5) and $P > 1000$ mm in Australia and $P > 1500$ mm in Africa (Figures S7 and S8 in Supporting Information S1). However, for $P < 400$ mm, *FSize* has a strong positive relationship with *P*, which can be explained by the low biomass accumulation rate in dry regions. Infrequent years with higher than usual rainfall can promote large fires in the following year (Bradstock, 2010), specifically in Australia, where *P_Var* and *FSize* had a positive linear relationship. The single most important predictor of *FSize* in Africa was *P_SI*, whereas *Temp* explained the most variation in *FSize* distribution in Australia. A drastic increase in the size of fires was observed when *Temp* >19°C.

In contrast, the relationship between *FRP* and the environmental variables was distinctly different in Africa and Australia. In Australia, similar to Murphy et al. (2013), interrelations between *FRP* and *BA* were identified. Very intense fires were observed under a variety of climate conditions, with the exception of regions experiencing high *P_Amp*, where in general high *BA* and low *FRP* were observed (Figure 5). In contrast, this relationship was not observed in Africa: intense fires could be found in most regions except tropical forests (i.e., the region with low *P_SI* and high *Tree)*. Arguably, the lack of a long, distinct season with conditions conducive to fire in the African tropical forests limits not only *BA* but also *FRP*. Additionally, a strong positive relationship was observed between *FRP* and *P* at the lower end of the precipitation gradient ($P < 1000$ mm). *P_Var* and *P_SI* showed the opposite pattern; while *P_Var* negatively affects *FRP*, *P_SI* promoted intense fires in Africa.

It should be noticed that, while the overall relationships between fire metrics and environmental variables were similar, the domain of the environmental space of fire regions differs between the two continents, as evident when comparing the range of the *x*-axes of the plots in Figure S7 in Supporting Information S1 with those of Figure S8 in Supporting Information S1. Likewise, fire regions were significantly different in terms of summary values of at least one of the fire metrics, as confirmed by Wilcoxon signed-rank tests (Table 2). As an illustrative example, we compared fire activity and environmental space of *Tropical Savannas* and *Deserts and Xeric Shrublands*, that is, two biomes with significant fire activity both in Africa and in Australia. Australian *Tropical Savannas* support lower tree cover (*Tree* = 8.5% vs. *Tree* = 20% in Africa), receive a lower annual rainfall (*P* = 976 and 1,208 mm in Australia and Africa, respectively) and experience higher precipitation variability (*P_Var* = 0.26 and 0.11 respectively). And while *Tropical Savannas* in the two continents experience similarly very large annual burned area (*BA* = 25% in regions 321–331 and 111–112), *FRP* and especially *FSize* were significantly higher

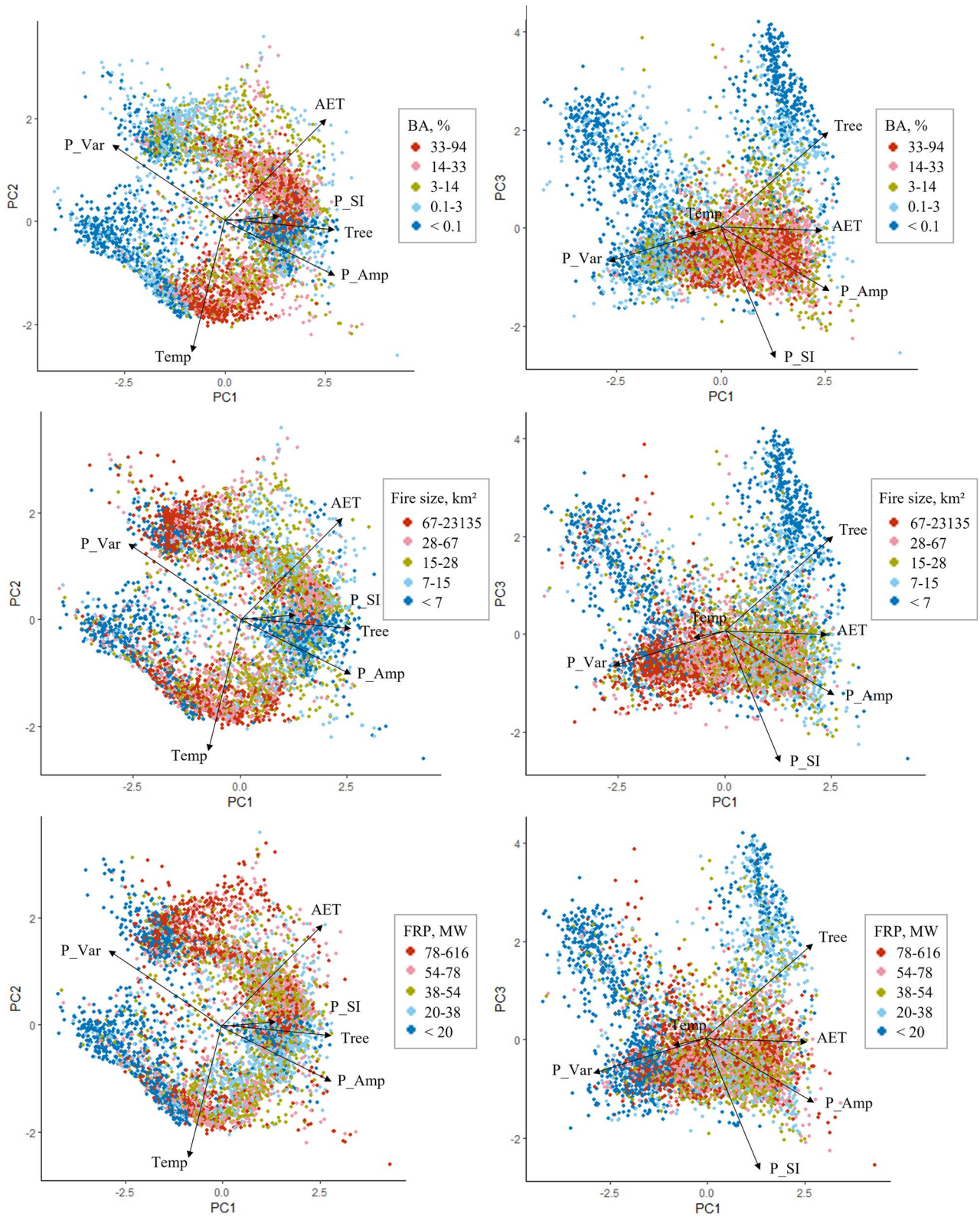

Figure 4. Characterization of the fire activity metrics in Africa within the space of the environmental variables: mean annual burned area (top), Fire size (middle), fire radiative power (bottom). Biplots show the ordination of 0.5° cells along the first and second principal components (PC) (left) and first and third PC (right). The points are plotted with a color scale indicating the value of the fire metric within the 0.5° cell, quantized by quintiles of the distribution of the metric values within the continent.

21698961, 2022, 8, Downloaded from https://agupubs.onlinelibrary.wiley.com/doi/10.1029/2021JG006694 by University Of Maryland, Wiley Online Library on [27/09/2023]. See the Terms and Conditions (https://onlinelibrary.wiley.com/terms-and-conditions) on Wiley Online Library for rules of use; OA articles are governed by the applicable Creative Commons License

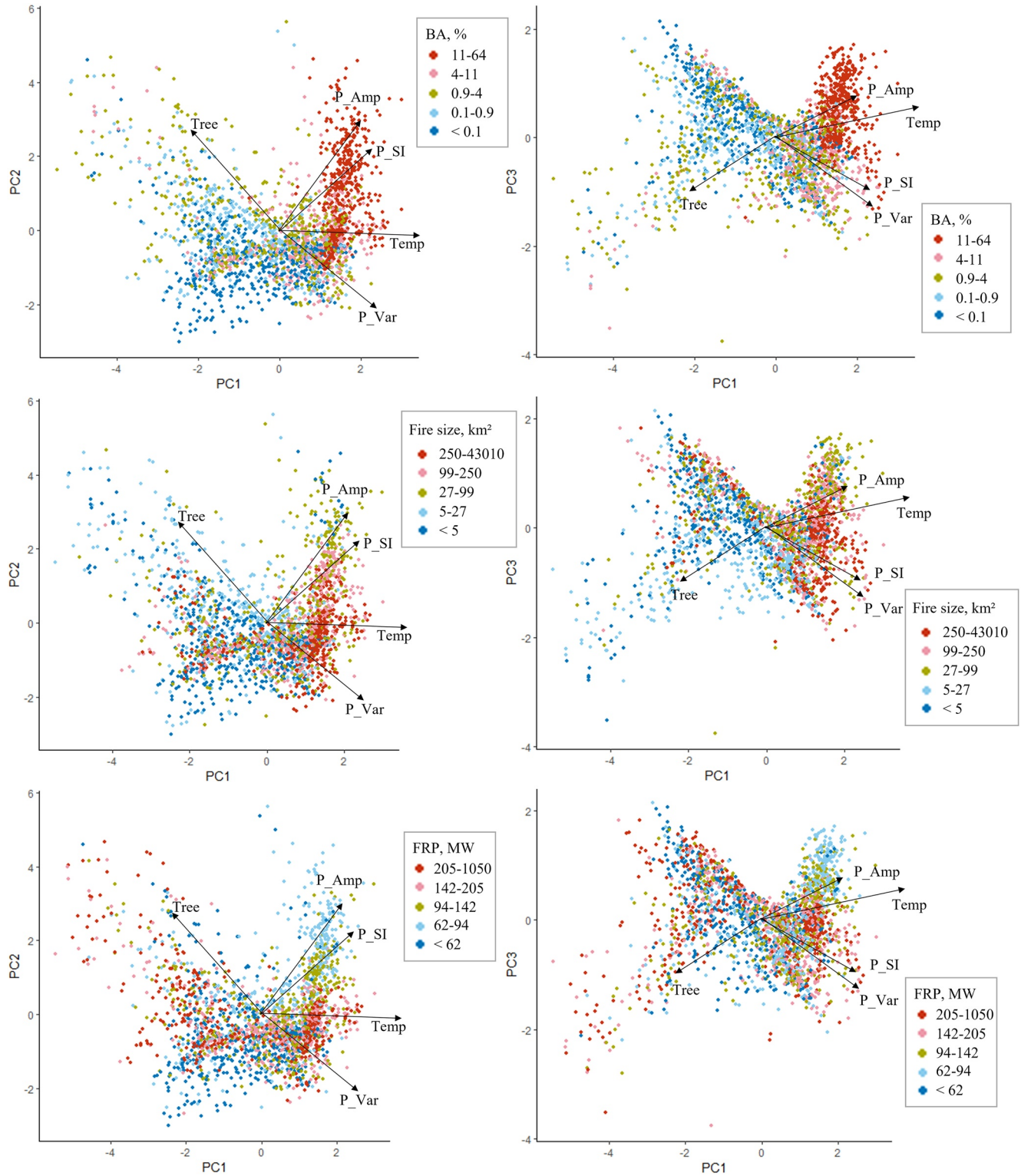

Figure 5. Characterization of the fire activity metrics in Australia within the space of the environmental variables: mean annual burned area (top), Fire size (middle), fire radiative power (bottom). Biplots show the ordination of 0.5° cells along the first and second principal components (PC) (left) and first and third PC (right). The points are plotted with a color scale indicating the value of the fire metric within the 0.5° cell, quantized by quintiles of the distribution of the metric values within the continent.

21698961, 2022, 8, Downloaded from https://agupubs.onlinelibrary.wiley.com/doi/10.1029/2021JG006694 by University Of Maryland, Wiley Online Library on [27/09/2023]. See the Terms and Conditions (https://onlinelibrary.wiley.com/terms-and-conditions) on Wiley Online Library for rules of use; OA articles are governed by the applicable Creative Commons License

21698961, 2022, 8, Downloaded from https://agupubs.onlinelibrary.wiley.com/doi/10.1029/2021JG006694 by University Of Maryland, Wiley Online Library on [27/09/2023]. See the Terms and Conditions (https://onlinelibrary.wiley.com/terms-and-conditions) on Wiley Online Library for rules of use; OA articles are governed by the applicable Creative Commons License

Table 2
Summary Values of the Three Fire Metrics, Calculated for Each Fire Region in Africa and Australia

Africa				
ID	Description	BA [%]	Fire size [km^2]	FRP [MW]
311	R-S-C	2.80*	18.67*	44.65*
321	F-S-I	19.86	24.90*	76.66*
322	F-S-I	25.19	27.91*	66.35*
323	F-S-I	19.72	31.77	61.27*
331	F-I-I	28.21	46.37	69.69*
332	I-I-I	8.35	59.89[a]	74.28
341	I-I-I	11.15[a]	45.72	83.14
342	R-L-H	3.97	204.14[a]	121.39*
351	R-S-I	1.08*	29.41	70.99*
Australia				
ID	Description	BA [%]	Fire Size [km^2]	FRP [MW]
111	F-L-I	22.33[a]	364.71[a]	107.33*
112	F-I-C	33.48*	114.88[a]	79.02*
121	I-L-H	7.86*	771.53*	195.48*
122	R-L-I	2.00	388.32*	171.56*
123	R-I-C	3.42[a]	99.24*	88.76*
131	R-I-I	1.02*	174.09*	175.14*
132	R-S-I	0.92	23.61*	152.12*
141	R-I-H	1.73	75.02*	208.31*

Note. *BA*: mean annual burned area; *FSize*: 95th percentile of the fire size distribution; *FRP*: 95th percentile of fire radiative power distribution. Abbreviations in the description: F—frequent, R—rare (in terms of *BA*), L—large, S—small (in terms of *FSize*), H—hot, C—cold (in terms of *FRP*), I—intermediate (for all fire metrics), similar to Archibald et al. (2013). It should be noted that high and low values of fire metrics were relative to each continent.

[a]Statistically different compared to other regions within the continent. *Statistically different compared to other regions between the continents, $p < 0.05$.

in Australia (Table 2). Differences in *FRP* and *FSize* were even more drastic between regions of the *Desert and Xeric Shrublands* biome (342 and 121–131), where fire activity in Australia is up to three times higher in terms of *FSize* and up to 1.5 times in terms of *FRP*. As in *Tropical Savannas*, *Deserts and Xeric Shrublands* in Australia occupy a portion of the environmental space with lower *P* (324 mm), higher *P_Var* (0.32), and higher *Temp* (22.7°C) compared to Africa (355 mm, 0.27, and 21.4°C, respectively).

4.2.2. Within-Region Anthropogenic Influence on Fire Activity

While the primary goal of this work was to delineate broad fire regions based on similar environmental conditions that shape fire activity, a simplistic analysis of human factors was included to demonstrate the potential use of the defined fire regions to study more local drivers of fire activity.

Overall, the analysis of the effect of anthropogenic pressure on fire activity metrics within the fire regions (Figure 2c, Table 3) confirmed the findings of previous studies: except for tropical forests where fire metrics increased with human pressure—consistent with fires in this region being tied with deforestation (Hoffmann et al., 2003)—we observed a negative relationship between fire activity and anthropogenic pressure (Archibald, 2016; Le Page et al., 2010; van Langevelde et al., 2003). Interestingly, our analysis showed that humans could exacerbate or minimize the variation in fire activity between two continents. For example, the drastic difference in *FSize* between the *Deserts and Xeric Shrublands* regions in Africa and Australia could be attributed to differences in the magnitude of anthropogenic pressure between the two continents since areas with a negligible level of human impact within the two fire regions show similar *FSize* (regions 342 and 122). In contrast, the difference in average *BA* in *Tropical Savannas* regions between two continents, which are overall small, substantially increased when

21698961, 2022, 8, Downloaded from https://agupubs.onlinelibrary.wiley.com/doi/10.1029/2021JG006694 by University Of Maryland, Wiley Online Library on [27/09/2023]. See the Terms and Conditions (https://onlinelibrary.wiley.com/terms-and-conditions) on Wiley Online Library for rules of use; OA articles are governed by the applicable Creative Commons License

Table 3
Mean Value of the Three Fire Metrics, Computed for Each Fire Region in Africa and Australia, Stratified by Human Pressure Level

Africa

Region	BA, %			Fire size, km^2			FRP, MW		
	Low human impact	Medium human impact	High human impact	Low human impact	Medium human impact	High human impact	Low human impact	Medium human impact	High human impact
311	2.06	5.76	5.52	16.53	27.26	19.32	44.00	44.02	58.71
321	21.07	10.95	–	25.33	16.96	–	79.53	46.46	–
322	27.96	13.88	16.72	31.77	18.68	18.03	66.79	63.12	62.06
323	24.29	17.48	5.61	33.27	30.05	26.52	60.22	66.42	33.62
331	42.95	23.04	8.07	62.68	33.70	23.61	71.87	64.70	55.42
332	7.77	10.11	3.56	77.06	51.73	37.57	83.14	62.01	50.96
341	20.98	8.19	2.71	65.47	26.62	30.70	87.19	79.19	59.81
342	3.91	4.50	–	386.94	27.05	–	125.66	103.36	–
351	0.74	2.72	0.71	36.06	20.82	32.20	72.26	66.36	82.69

Australia

Region	BA, %		Fire Size, km^2		FRP, MW	
	Low human impact	Medium/High human impact	Low human impact	Medium/High human impact	Low human impact	Medium/High human impact
111	22.99	1.09	403.77	111.22	107.38	81.69
112	33.48	–	114.88	–	79.02	–
121	7.97	1.11	786.30	51.83	195.77	157.08
122	2.00	–	388.32	–	171.56	–
123	4.99	2.22	201.14	45.29	92.17	85.79
131	1.21	0.50	610.28	10.73	199.39	90.75
132	1.13	0.87	615.13	17.39	294.62	119.10
141	2.50	1.49	146.24	44.35	242.15	195.17

only low human pressure areas were considered. In other words, in the absence of humans, *Tropical Savannas* in Africa support more frequent fires than in Australia. It is also important to state that while, based on previous research, it was expected that humans drastically alter fire activity, our analysis showed that the magnitude of human influences varied substantially across biomes. For instance, both regions 132 (mostly *Mediterranean* and *Temperate Forests* in Southwestern and Southeastern Australia) and 341 (mostly Montane Grassland and Tropical Savannas, both North and South of the Equator in Africa) encompass mostly human-managed lands and therefore experience a very high level of anthropogenic pressure (Figure S2 in Supporting Information S1). The high proportion of croplands and high livestock density has, however, a different impact on fire metrics in the two regions. High levels of human pressure substantially decreased *BA* in region 341 but had a low impact on *Fsize* and *FRP*, whereas, in region 132, high human pressure had a more severe impact on *FSize* and *FRP* than *BA*.

5. Discussion

5.1. Correspondence Between Fire Regions, Biomes and Climate Zones

The spatial distribution of the fire regions (Figure 3) shares some similarities with the terrestrial biomes defined by Olson et al. (2001) and the Köpper-Geiger climate classification (KG, Kottek et al., 2006), which is not surprising since climate data are one of the main inputs of all three maps. However, biomes were delineated based on similar climate and vegetation cover that support the distribution of selected groups of plants and animals. In contrast, fire regions were defined as areas homogeneous in terms of environmental conditions that promote fuel accumulation and desiccation (i.e., fire potential). As a result, a number of dissimilarities can be recognized

between the spatial distribution of biomes and fire regions. First, similar to the KG map, the tropical savannas biome was split into several regions to represent the full spectrum of biophysical conditions and fire activity. While the *P* in Australia has a distinct Northeast to Southwest gradient (evident in the KG map), the gradient of *BA* follows the North-South direction and *FSize* the West-East one. The patterns are captured by the fire regions: the *Tropical Savannas* biome is split into a Northern tropical region (112) with the highest *BA*, a Northern arid region (111) with high *BA* and high *FSize*, and an Eastern region (123) with drastically lower *BA*. The *Tropical Savannas* biome in Africa was split into two regions North of the equator (323, 331) and two South of the equator (321, 322). This split is driven by the spatial pattern of *Tree*, which negatively affects *BA*, as reported above. Additionally, while the Sahel and the Horn of Africa also belong to the *Tropical Savannas* biome, they experience different climates. Consequently, they were separated into region 332 (Sahel) with the lowest *Tree* in Africa, lower *BA* and higher *FSize* compared to other tropical savannas regions (321–331), and region 351 (Horn of Africa), which had the lowest *P_SI* in both continents and the lowest *BA* in Africa.

In Australia, the *Deserts and Xeric Shrublands* biome is also assigned to a single climatic zone by KG, but it experiences a large gradient of *BA* and *FSize*. This biome was split into three fire regions, roughly along the North-South direction, corresponding to progressively higher *FSize* and lower *BA*. The Northern region (121) had the largest *FSize*, whereas regions 122 and 131 had significantly lower *FSize* and *BA*. *FRP* remained high in all arid regions.

In Africa, as in KG, the *Montane Grasslands* and Southern part of the *Tropical Savannas* biomes were merged in a single region (fire region 341) with an intermediate level of fire activity between the rest of the *Tropical Savannas* and the fire regions encompassing *Deserts and Xeric Shrublands*. Meanwhile in Australia, *Mediterranean and Temperate Forests* showed similar fire activity, the lowest *BA* and *FSize*, possible due to high population density and a high proportion of human-managed land (Figure S2 in Supporting Information S1), which showed to substantially decrease the rate of fire spread (Archibald, 2016; Archibald et al., 2012; Le Page et al., 2010; Mouillot & Field, 2005). Therefore, both biomes were assigned to one fire region (132) except for Tasmania and a small southwest part of the mainland with a temperate, dry and warm summer climate (region 141) that showed higher *FSize* and *FRP* than in region 132.

5.2. Comparison of the Fire Regions to Published Fire Regimes Maps

Despite the importance of fire regimes delineation, only two global fire regimes maps are currently available in the peer revied literature. Chuvieco et al. (2008) defined eight fire regimes based on levels of fire frequency and its inter-and intra-annual variability, whereas Archibald et al. (2013) used the clustering of *BA*, *FSize*, and *FRP* to define five key global fire regimes. Similar to our results, both studies distinguished some variation in fire activity between the *Tropical Savannas* in Africa and Australia (Figure S12 in Supporting Information S1). In the *Desert and Xeric Shrublands* biome, however, the two global fire regimes map were not able to distinguish drastic differences in fire activity between Africa and Australia, which we found to vary significantly in terms of *FSize* and *FRP*. Additionally, Archibald et al. (2013) identified similar fire regimes in temperate grasslands in Australia and tropical forests in Africa, while our results indicate that those two regions differ significantly, especially in terms of *FRP*.

In short, previous efforts to map global fire regimes often failed to differentiate between regions with significant variation in one or more fire-regime metrics and combined several biomes with different environmental conditions (e.g., fuel-limited and energy-limited) into one fire regime. One possible explanation is the a priori choice of the number of global fire regimes, which might be insufficient to represent the variety of fire activity between and within continents. For example, in contrast to our findings, Archibald et al. (2013) failed to observe any clear relationship between delineated fire regimes and climate variables or biomes.

It is also important to acknowledge that the opposite of our fire regions, previously mentioned maps of fire regimes were restricted by the length of the fire record, which was limited to 6 years for Chuvieco et al. (2008) and 14 years for Archibald et al. (2013). The lack of fire detections in places with moderate to low-frequency fire return intervals impeded assigning a fire regime to many parts of the world, which can be misinterpreted as an absence of fire activity. Therefore, existing fire regime maps based on a few fire metrics cannot be utilized for their main purpose, such as understanding what processes shape current fire activity.

21698961, 2022, 8, Downloaded from https://agupubs.onlinelibrary.wiley.com/doi/10.1029/2021JG006694 by University Of Maryland, Wiley Online Library on [27/09/2023]. See the Terms and Conditions (https://onlinelibrary.wiley.com/terms-and-conditions) on Wiley Online Library for rules of use; OA articles are governed by the applicable Creative Commons License

21698961, 2022, 8, Downloaded from https://agupubs.onlinelibrary.wiley.com/doi/10.1029/2021JG006694 by University Of Maryland, Wiley Online Library on [27/09/2023]. See the Terms and Conditions (https://onlinelibrary.wiley.com/terms-and-conditions) on Wiley Online Library for rules of use; OA articles are governed by the applicable Creative Commons License

To incorporate fire-climate relationships into fire regime mapping, similar to our approach, several previous studies analyzed changes in fire metrics across environmental gradients. However, by selecting one rather than a set of environmental variables, those studies could not recognize the variety of fire regimes across biomes. For example, Hantson et al. (2017) detected a drastic reduction in *FSize* in the tropics once *P* reaches 550 m due to an increase in tree cover and concluded that dry tropical regions experience larger, hotter, and more rare fires compared to wet tropics. While overall, it is a fair statement, we showed that *FSize* and *FRP* are not always higher in dry tropics compared to the wet (e.g., the Horn of Africa vs. tropical savannas), and not all wet tropical regions experience higher *BA* than dry regions (e.g., tropical forest vs. Sahel or desert and xeric shrublands in Africa). Additionally, based on our GAMs, we found that *P* threshold for *FSize* reduction was much higher, 1000 mm in Australia and 1500 mm in Africa (Figures S7 and S8 in Supporting Information S1).

Recognizing a variety of fire regimes within one continent and their strong connection with moisture, Russell-Smith et al. (2007) defined 10 regions in Australia using seasonal rainfall distribution. We similarly found that *P_Amp* and *P_SI* were important predictors of fire activity in Australia, especially for *BA*, and a certain resemblance between our fire regions and Russell-Smith's rainfall classes can be recognized. However, by including other environmental variables in our classification, we were able to define regions statistically different not only in terms of *BA* but also *FSize* and *FRP*. We found that *FSize* and *FRP* do not follow a precipitation gradient as closely as *BA*; therefore, rainfall seasonality alone cannot explain the complexity of the fire phenomenon and account for multiple processes that drive fire (Bradstock, 2010).

We finish our comparison by acknowledging the work of Murphy et al. (2013) that described in great detail broad fire regimes in Australia also using environmental controls of fire activity, such as major fuel types and climatic domains, as a baseline. The comparison between the fire regions and Murphy's map revealed that our regions somewhat captured the overall spatial pattern of fire frequency and intensity in Australia. However, instead of using statistical analysis to delineate fire regions, Murphy et al. (2013) used experts' opinions and local literature. While we do not dispute that local knowledge can enhance our understanding of the spatial distribution of historical and modern fire activity, it can also bring a certain degree of subjectivity, bias, and a lack of reproducibility to the method.

5.3. Limitations of the Study

Some limitations must be considered in interpreting the results of the proposed approach. First, while the potential drivers of fire activity used in this study were identified through a thorough literature review, not all potential fire climatic and environmental drivers were considered. Other variables such as wind and fire-weather indices that can reflect short-term dry spells can potentially explain some discrepancies between climate domains and fire metrics (Abatzoglou & Kolden, 2013; Archibald et al., 2009). Moreover, while elevation, aspect, slope, soil properties, fuel types, ignitions, and fire management practices can have a profound effect on different fire characteristics (Archibald et al., 2009; Russell-Smith et al., 2007; Stevens et al., 2017), their impact might be too local for the scope of this paper. It is also worth mentioning that while only a few variables (6 in Africa, 5 in Australia) were used in the PCA and clustering analysis, strong collinearity between many of the environmental variables might preclude the identification of the single most important driver—caution is therefore recommended if the results of this study were to be used in physically-based fire models.

Second, this study is limited by the quality of currently available remotely sensed data. In particular, the MODIS fire products do not capture small, low-intensity fires (Boschetti et al., 2019; Kumar et al., 2011), which could, in some fire regions, introduce biases in the fire activity metrics. This issue is particularly relevant in frequently burned environments and within highly managed lands (Laris, 2005), thus fire-data limitations could affect the results of the anthropogenic pressure analysis, spuriously restricting it to bigger fires. Recent studies by Roy et al. (2019) and Ramo et al. (2021) demonstrated the severe underestimation of small fires in Africa by the MCD64A1 product, especially within cropland and savannas. Additionally, coarse resolution land cover products fail to detect small agricultural fields, which are prevalent in Africa (Inglada et al., 2015; Midekisa et al., 2017) and can be used as fire breaks, increasing landscape fragmentation. Meanwhile, precipitation datasets are less accurate in regions with inadequate rain gauge network (Dinku et al., 2014; Toté et al., 2015).

Third, while remotely sensed data is the only source for global analysis to capture spatial and temporal patterns of fire activity (Benali et al., 2017), there is no agreement on the minimum fire record length required to adequately

21698961, 2022, 8, Downloaded from https://agupubs.onlinelibrary.wiley.com/doi/10.1029/2021JG006694 by University Of Maryland, Wiley Online Library on [27/09/2023]. See the Terms and Conditions (https://onlinelibrary.wiley.com/terms-and-conditions) on Wiley Online Library for rules of use; OA articles are governed by the applicable Creative Commons License

capture the inter-annual variability in fire activity, especially in places with moderate to low-frequency fire return interval (Bowman et al., 2009; Daniau et al., 2012; Krawchuk & Moritz, 2014). And only a limited number of fire metrics can be currently estimated from remote-sensed data. Some essential components of the fire regime concept, for example, fire type and severity, were omitted in this study.

Fourth, some aspects of the statistical analysis add uncertainty. For instance, the selection of the number of clusters through inspection of the dendrogram is rather arbitrary; a lower or higher number of fire regions might more preferable depending on the scale of analysis and on the intended use of the ecoregions. We note, however, that the hierarchical clustering provides a straightforward aggregation of the fire regions: using the first two digits of the fire region ID results in a rigorously defined coarser map. Additionally, there are issues with the separability of some of the clusters: Figure 2 shows a certain degree of overlap between clusters and a number of cells close to the decision boundary.

Finally, the aggregation of 0.5° cells into ecoregions also resulted in the loss of some local-scale features. This is evident in Ethiopia, a highly diverse country that encompasses 11 different ecoregions, where cells belonging to 7 different fire regions were primarily merged into two major regions (341, 351) with a few cells merged into regions 311, 331, and 332.

These limitations notwithstanding, the methods presented in this paper are general ones. We would advocate that, for local studies, smaller than a country level, a user can adopt the proposed approach to define more refine fire regions using data from local weather stations, field data, and higher resolution imagery to avoid some of the biases and limitations of coarser resolution data.

6. Conclusions

This study proposed a new approach for mapping the diversity of potential fire activity at the continental level, based on key processes that control fuel accumulation, desiccation, and fire propagation. One of the advantages of the proposed method is that the fire regions were identified through the statistical analysis of climate and environmental variables reflecting broad biophysical processes rather than using observed fire activity metrics as input data – unlike previous studies that have used a limited set of metrics estimated over short time periods (e.g., Archibald et al., 2013; Chuvieco et al., 2008; Le Page et al., 2008). Furthermore, the analysis was conducted separately for each continent, without the implicit assumption that the same "fire regime" exists in different continents. Reflecting the heterogeneity of fire characteristics within biomes and between continents, the proposed methods resulted in 9 and 8 regions in Africa and Australia, with distinct climate, vegetation, and fire activity.

Fire activity metrics computed from the 2002–2019 record of the global MODIS satellite fire record were used to characterize the fire activity level of each region, thus evaluating the effectiveness of the proposed fire region map. We found that different environmental variables act as key limiting factors for fire activity in Africa and Australia. Consistently with the current fire ecology literature (Chuvieco et al., 2021; Lehmann et al., 2014), temperature was found to be a more important predictor of fire activity (especially for the average annual burned area and the fire size) in Australia than in Africa, whereas precipitation and the highly correlated tree cover were the primary predictors of *BA* and fire intensity (*FRP)* in Africa.

We believe that delineated fire regions can be used not only as a spatial unit for calculating fire statistics but also to study how changes in fire drivers could reshape fire activity in the future and to analyze anthropogenic drivers of fire within regions homogeneous in terms of climate controls. In this study, we demonstrated that humans' potential to transform a different aspect of fire activity varied within climate space; therefore, any attempt to generalize the human-fire relationship at the continental or global scale will severely oversimplify the role of humans in shaping modern fire activity. Ultimately, while our understanding of broad-scale fire-climate relationships is improving, more research is needed to evaluate the impacts of socio-economic factors on those relationships, particularly in tropics where climate- or human-related changes in fire activity could also drive long-term changes in vegetation composition since fire is one of the main controls of grass-forest coexistence (Lehmann et al., 2014; Sankaran et al., 2005).

Data Availability Statement

The observational datasets used in this study are freely available. MCD64A1: https://lpdaac.usgs.gov/products/mcd64a1v006/. MCD14ML: https://firms.modaps.eosdis.nasa.gov/download/. FLDAS: https://disc.gsfc.nasa.gov/datasets?keywords=FLDAS%26page=1. TERRACLIMATE: http://www.climatologylab.org/terraclimate.html. CCI LC: http://maps.elie.ucl.ac.be/CCI/viewer/download.php. MOD44B: https://modis.gsfc.nasa.gov/data/dataprod/mod44.php. Global Aboveground and Belowground Biomass Carbon Density: https://doi.org/10.3334/ORNLDAAC/1763. Ecoregions: https://www.worldwildlife.org/publications/terrestrial-ecoregions-of-the-world. Livestock: https://dataverse.harvard.edu/dataset.xhtml?persistentId=doi:10.7910/DVN/GIVQ75. Population density: https://sedac.ciesin.columbia.edu/data/collection/gpw-v4. All statistical analyses were performed in R 4.1.2 (R Core Team, 2017). The R *mgcv* package (v.1.8.38; Wood & Wood, 2017) was used for GAM (function *gam*), and the *stats* package (v.1.4.2; R Core Team, 2017) was used for PCA and clustering (functions *prcomp* and *hclust*, respectively). The maps of fire regions and R code from this study can be obtained from Zenodo (https://doi.org/10.5281/zenodo.6646835).

Acknowledgments
This work was supported by NASA awards 80NSSC18K0739 and 80NSSC18K0400.

References

Abatzoglou, J. T., Dobrowski, S. Z., Parks, S. A., & Hegewisch, K. C. (2018). Terraclimate, a high-resolution global dataset of monthly climate and climatic water balance from 1958-2015. *Scientific Data*, *5*(1), 170191. https://doi.org/10.1038/sdata.2017.191

Abatzoglou, J. T., & Kolden, C. A. (2013). Relationships between climate and macroscale area burned in the western United States. *International Journal of Wildland Fire*, *22*(7), 1003. https://doi.org/10.1071/WF13019

Abatzoglou, J. T., Redmond, K. T., & Edwards, L. M. (2009). Classification of regional climate variability in the state of California. *Journal of Applied Meteorology and Climatology*, *48*(8), 1527–1541. https://doi.org/10.1175/2009JAMC2062.1

Abatzoglou, J. T., Williams, A. P., Boschetti, L., Zubkova, M., & Kolden, C. A. (2018). Global patterns of interannual climate–fire relationships. *Global Change Biology*, *24*(11), 5164–5175. https://doi.org/10.1111/gcb.14405

Aldersley, A., Murray, S. J., & Cornell, S. E. (2011). Global and regional analysis of climate and human drivers of wildfire. *Science of the Total Environment*, *409*(18), 3472–3481. https://doi.org/10.1016/j.scitotenv.2011.05.032

Allen, R. G., Pereira, L. S., Raes, D., & Smith, M. (1998). Crop evapotranspiration-Guidelines for computing crop water requirements-FAO Irrigation and drainage paper 56. *FAO*, *300*(9), D05109.

Archibald, S. (2016). Managing the human component of fire regimes: Lessons from Africa. *Philosophical Transactions of the Royal Society B Biological Sciences*, *371*(1696), 20150346. https://doi.org/10.1098/rstb.2015.0346

Archibald, S., Lehmann, C. E. R., Gómez-Dans, J. L., & Bradstock, R. A. (2013). Defining pyromes and global syndromes of fire regimes. *Proceedings of the National Academy of Sciences*, *110*(16), 6442–6447. https://doi.org/10.1073/pnas.1211466110

Archibald, S., Nickless, A., Govender, N., Scholes, R. J., & Lehsten, V. (2010). Climate and the inter-annual variability of fire in southern Africa: A meta-analysis using long-term field data and satellite-derived burnt area data. *Global Ecology and Biogeography*, *19*(6), 794–809. https://doi.org/10.1111/j.1466-8238.2010.00568.x

Archibald, S., Roy, D. P., Wilgen, B. W. V., & Scholes, R. J. (2009). What limits fire? An examination of drivers of burnt area in Southern Africa. *Global Change Biology*, *15*(3), 613–630. https://doi.org/10.1111/j.1365-2486.2008.01754.x

Archibald, S., Staver, A. C., & Levin, S. A. (2012). Evolution of human-driven fire regimes in Africa. *Proceedings of the National Academy of Sciences*, *109*(3), 847–852. https://doi.org/10.1073/pnas.1118648109

Benali, A., Mota, B., Carvalhais, N., Oom, D., Miller, L. M., Campagnolo, M. L., & Pereira, J. M. C. (2017). Bimodal fire regimes unveil a global-scale anthropogenic fingerprint. *Global Ecology and Biogeography*, *26*(7), 799–811. https://doi.org/10.1111/geb.12586

Boer, M. M., Bowman, D. M. J. S., Murphy, B. P., Cary, G. J., Cochrane, M. A., Fensham, R. J., et al. (2016). Future changes in climatic water balance determine potential for transformational shifts in Australian fire regimes. *Environmental Research Letters*, *11*(6), 065002. https://doi.org/10.1088/1748-9326/11/6/065002

Bonetti, M. F., & Wiens, J. J. (2014). Evolution of climatic niche specialization: A phylogenetic analysis in amphibians. *Proceedings of the Royal Society*, *281*(1795), 20133229. https://doi.org/10.1098/rspb.2013.3229

Boschetti, L., & Roy, D. P. (2008). Defining a fire year for reporting and analysis of global interannual fire variability. *Journal of Geophysical Research*, *113*(G3), G03020. https://doi.org/10.1029/2008JG000686

Boschetti, L., Roy, D. P., Giglio, L., Huang, H., Zubkova, M., & Humber, M. L. (2019). Global validation of the collection 6 MODIS burned area product. *Remote Sensing of Environment*, *235*, 111490. https://doi.org/10.1016/j.rse.2019.111490

Bowman, D. M. J. S., Balch, J. K., Artaxo, P., Bond, W. J., Carlson, J. M., Cochrane, M. A., et al. (2009). Fire in the Earth system. *Science*, *324*(5926), 481–484. https://doi.org/10.1126/science.1163886

Bradstock, R. A. (2010). A biogeographic model of fire regimes in Australia: Current and future implications. *Global Ecology and Biogeography*, *19*(2), 145–158. https://doi.org/10.1111/j.1466-8238.2009.00512.x

CCI-LC-PUGV2. (2017). Land cover CCI product user guide version 2.0.

Chen, D., Pereira, J. M. C., Masiero, A., & Pirotti, F. (2017). Mapping fire regimes in China using MODIS active fire and burned area data. *Applied Geography*, *85*, 14–26. https://doi.org/10.1016/j.apgeog.2017.05.013

Christopoulos, D. T. (2016). Introducing Unit Invariant Knee (UIK) as an objective choice for elbow point in multivariate data analysis techniques. *Available at SSRN 3043076 Electronic Journal*. https://doi.org/10.2139/ssrn.3043076

Chuvieco, E., Giglio, L., & Justice, C. (2008). Global characterization of fire activity: Toward defining fire regimes from Earth observation data. *Global Change Biology*, *14*(7), 1488–1502. https://doi.org/10.1111/j.1365-2486.2008.01585.x

Chuvieco, E., Pettinari, M. L., Koutsias, N., Forkel, M., Hantson, S., & Turco, M. (2021). Human and climate drivers of global biomass burning variability. *Science of the Total Environment*, *779*, 146361. https://doi.org/10.1016/j.scitotenv.2021.146361

CIESIN. (2016). Center for International Earth Science Information Network - CIESIN - Columbia University. *Gridded population of the world, version 4 (GPWv4): Data quality indicators*. NASA Socioeconomic Data and Applications Center (SEDAC). https://doi.org/10.7927/H49C6VBN

Cochrane, M. A. (2003). Fire science for rainforests. *Nature*, *421*(6926), 913–919. https://doi.org/10.1038/nature01437

21698961, 2022, 8, Downloaded from https://agupubs.onlinelibrary.wiley.com/doi/10.1029/2021JG006694 by University Of Maryland, Wiley Online Library on [27/09/2023]. See the Terms and Conditions (https://onlinelibrary.wiley.com/terms-and-conditions) on Wiley Online Library for rules of use; OA articles are governed by the applicable Creative Commons License

Conedera, M., Krebs, P., Valese, E., Cocca, G., Schunk, C., Menzel, A., et al. (2018). Characterizing Alpine pyrogeography from fire statistics. *Applied Geography*, *98*, 87–99. https://doi.org/10.1016/j.apgeog.2018.07.011

Daniau, A.-L., Bartlein, P. J., Harrison, S. P., Prentice, I. C., Brewer, S., Friedlingstein, P., et al. (2012). Predictability of biomass burning in response to climate changes. *Global Biogeochemical Cycles*, *26*(4), GB4007. https://doi.org/10.1029/2011GB004249

DiMiceli, C. M., Carroll, M. L., Sohlberg, R. A., Huang, C., Hansen, M. C., & Townshend, J. R. G. (2017). *Annual global automated MODIS vegetation continuous fields (MOD44B) at 250 m spatial resolution for data years beginning day 65, 2000–2014, collection 5 percent tree cover, version 6*. University of Maryland.

Dinku, T., Hailemariam, K., Maidment, R., Tarnavsky, E., & Connor, S. (2014). Combined use of satellite estimates and rain gauge observations to generate high-quality historical rainfall time series over Ethiopia. *International Journal of Climatology*, *34*(7), 2489–2504. https://doi.org/10.1002/joc.3855

Faivre, N., Roche, P., Boer, M. M., McCaw, L., & Grierson, P. F. (2011). Characterization of landscape pyrodiversity in Mediterranean environments: Contrasts and similarities between south-Western Australia and south-eastern France. *Landscape Ecology*, *26*(4), 557–571. https://doi.org/10.1007/s10980-011-9582-6

Flannigan, M. D., Krawchuk, M. A., de Groot, W. J., Wotton, B. M., & Gowman, L. M. (2009). Implications of changing climate for global wildland fire. *International Journal of Wildland Fire*, *18*(5), 483–507. https://doi.org/10.1071/WF08187

Funk, C., Peterson, P., Landsfeld, M., Pedreros, D., Verdin, J., Shukla, S., et al. (2015). The climate hazards infrared precipitation with stations—A new environmental record for monitoring extremes. *Scientific Data*, *2*(1), 150066. https://doi.org/10.1038/sdata.2015.66

Giglio, L. (2013). MODIS collection 5 active fire product user's guide version 2.5 61.

Giglio, L., Boschetti, L., Roy, D. P., Humber, M. L., & Justice, C. O. (2018). The Collection 6 MODIS burned area mapping algorithm and product. *Remote Sensing of Environment*, *217*, 72–85. https://doi.org/10.1016/j.rse.2018.08.005

Giglio, L., Loboda, T., Roy, D. P., Quayle, B., & Justice, C. O. (2009). An active-fire based burned area mapping algorithm for the MODIS sensor. *Remote Sensing of Environment*, *113*(2), 408–420. https://doi.org/10.1016/j.rse.2008.10.006

Giglio, L., Schroeder, W., & Justice, C. O. (2016). The collection 6 MODIS active fire detection algorithm and fire products. *Remote Sensing of Environment*, *178*, 31–41. https://doi.org/10.1016/j.rse.2016.02.054

Gilbert, M., Nicolas, G., Cinardi, G., Van Boeckel, T. P., Vanwambeke, S. O., Wint, G. R. W., & Robinson, T. P. (2018). Global distribution data for cattle, buffaloes, horses, sheep, goats, pigs, chickens and ducks in 2010. *Scientific Data*, *5*(1), 180227. https://doi.org/10.1038/sdata.2018.227

Gill, A. M. (1975). Fire and the Australian flora: A review. *Australian Forestry*, *38*(1), 4–25. https://doi.org/10.1080/00049158.1975.10675618

Gillett, N. P., Weaver, A. J., Zwiers, F. W., & Flannigan, M. D. (2004). Detecting the effect of climate change on Canadian forest fires. *Geophysical Research Letters*, *31*(18), L18211. https://doi.org/10.1029/2004GL020876

Girden, E. R. (2010). *Evaluating research articles from start to finish* (3rd edn.). SAGE Publications, Inc.

Guyette, R. P., Muzika, R. M., & Dey, D. C. (2002). Dynamics of an anthropogenic fire regime. *Ecosystems*, *5*, 472–486. https://doi.org/10.1007/s10021-002-0115-7

Hantson, S., Scheffer, M., Pueyo, S., Xu, C., Lasslop, G., Van Nes, E. H., et al. (2017). Rare, Intense, Big fires dominate the global tropics under drier conditions. *Scientific Reports*, *7*, 1–5. https://doi.org/10.1038/s41598-017-14654-9

Hoffmann, W. A., Jaconis, S. Y., Mckinley, K. L., Geiger, E. L., Gotsch, S. G., & Franco, A. C. (2012). Fuels or microclimate? Understanding the drivers of fire feedbacks at savanna– forest boundaries. *Austral Ecology*, *37*(6), 634–643. https://doi.org/10.1111/j.14429993.2011.02324.x

Hoffmann, W. A., Schroeder, W., & Jackson, R. B. (2003). Regional feedbacks among fire, climate, and tropical deforestation. *Journal of Geophysical Research*, *108*(D23), 4721. https://doi.org/10.1029/2003JD003494

Holt, R. D. (2009). Bringing the Hutchinsonian niche into the 21st century: Ecological and evolutionary perspectives. *Proceedings of the National Academy of Sciences*, *106*, 19659–19665. https://doi.org/10.1073/pnas.0905137106

Humber, M. L. (2019). *Towards object-based evaluation of individual fires at global scales [Doctoral dissertation]*. University of Maryland, ProQuest Dissertations Publishing. https://doi.org/10.13016/c6rt-bl6z

Hutchinson, G. E. (1957). Concluding remarks. Population studies: Animal ecology and demography. *Cold Spring Harbor Symposia on Quantitative Biology*, *22*(0), 415–457. https://doi.org/10.1101/sqb.1957.022.01.039

Inglada, J., Arias, M., Tardy, B., Hagolle, O., Valero, S., Morin, D., et al. (2015). Assessment of an operational system for crop type map production using high temporal and spatial resolution satellite optical imagery. *Remote Sensing*, *7*(9), 12356–12379. https://doi.org/10.3390/rs70912356

Jiang, H., & Eskridge, K. M. (2000). "Bias in principal component analysis due to correlated observations". In *Conference on applied statistics in agriculture*. https://doi.org/10.4148/2475-7772.1247

Jiménez-Ruano, A., Mimbrero, M. R., & de la Riva Fernández, J. (2017). Understanding wildfires in mainland Spain. A comprehensive analysis of fire regime features in a climate-human context. *Applied Geography*, *89*, 100–111. https://doi.org/10.1016/j.apgeog.2017.10.007

Kahiu, M. N., & Hanan, N. P. (2018). Fire in sub-Saharan Africa: The fuel, cure and connectivity hypothesis. *Global Ecology and Biogeography*, *27*(8), 946–957. https://doi.org/10.1111/geb.12753

Kottek, M., Grieser, J., Beck, C., Rudolf, B., & Rubel, F. (2006). World map of the Köppen-Geiger climate classification updated. *Meteorologische Zeitschrift*, *15*(3), 259–263. https://doi.org/10.1127/0941-2948/2006/0130

Krawchuk, M. A., & Moritz, M. A. (2011). Constraints on global fire activity vary across a resource gradient. *Ecology*, *92*(1), 121–132. https://doi.org/10.1890/09-1843.1

Krawchuk, M. A., & Moritz, M. A. (2014). Burning issues: Statistical analyses of global fire data to inform assessments of environmental change. *Environmetrics*, *25*(6), 472–481. https://doi.org/10.1002/env.2287

Krawchuk, M. A., Moritz, M. A., Parisien, M.-A., Dorn, J. V., & Hayhoe, K. (2009). Global pyrogeography: The current and future distribution of wildfire. *PLoS One*, *4*, e5102. https://doi.org/10.1371/journal.pone.0005102

Krebs, P., Pezzatti, G. B., Mazzoleni, S., Talbot, L. M., & Conedera, M. (2010). Fire regime: History and definition of a key concept in disturbance ecology. *Theory in Biosciences*, *129*(1), 53–69. https://doi.org/10.1007/s12064-010-0082-z

Kumar, S. S., Roy, D. P., Boschetti, L., & Kremens, R. (2011). Exploiting the power law distribution properties of satellite fire radiative power retrievals: A method to estimate fire radiative energy and biomass burned from sparse satellite observations. *Journal of Geophysical Research*, *116*(D19), D19303. https://doi.org/10.1029/2011jd015676

Laris, P. (2005). Spatiotemporal problems with detecting and mapping mosaic fire regimes with coarse-resolution satellite data in savanna environments. *Remote Sensing of Environment*, *99*(4), 412–424. https://doi.org/10.1016/j.rse.2005.09.012

Lavorel, S., Flannigan, M. D., Lambin, E. F., & Scholes, M. C. (2007). Vulnerability of land systems to fire: Interactions among humans, climate, the atmosphere, and ecosystems. *Mitigation and Adaptation Strategies for Global Change*, *12*(1), 33–53. https://doi.org/10.1007/s11027-006-9046-5

Lehmann, C. E. R., Anderson, T. M., Sankaran, M., Higgins, S. I., Archibald, S., Hoffmann, W. A., et al. (2014). Savanna vegetation-fire-climate relationships differ among continents. *Science*, *343*(6170), 548–552. https://doi.org/10.1126/science.1247355

21698961, 2022, 8, Downloaded from https://agupubs.onlinelibrary.wiley.com/doi/10.1029/2021JG006694 by University Of Maryland, Wiley Online Library on [27/09/2023]. See the Terms and Conditions (https://onlinelibrary.wiley.com/terms-and-conditions) on Wiley Online Library for rules of use; OA articles are governed by the applicable Creative Commons License

Lehmann, C. E. R., Archibald, S. A., Hoffmann, W. A., & Bond, W. J. (2011). Deciphering the distribution of the savanna biome. *New Phytologist*, *191*(1), 197–209. https://doi.org/10.1111/j.1469-8137.2011.03689.x

Le Page, Y., Oom, D., Silva, J. M. N., Jönsson, P., Pereira, J. M. C. (2010). Seasonality of vegetation fires as modified by human action: observing the deviation from eco-climatic fire regimes. *Global Ecology and Biogeography*. *19*, 575–588. https://doi.org/10.1111/j.1466-8238.2010.00525.x

Le Page, Y., Pereira, J. M. C., Trigo, R., Da Camara, C., Oom, D., & Mota, B. (2008). Global fire activity patterns (1996-2006) and climatic influence: An analysis using the World Fire Atlas. *Atmospheric Chemistry and Physics*, *8*(7), 1911–1924. https://doi.org/10.5194/acp-8-19112008

Leys, B. A., Marlon, J. R., Umbanhowar, C., & Vannière, B. (2018). Global fire history of grassland biomes. *Ecology and Evolution*, *8*(17), 8831–8852. https://doi.org/10.1002/ece3.4394

Loboda, T. V., Hall, J. V., Hall, A. H., & Shevade, V. S. (2017). *ABoVE: Cumulative annual burned area, circumpolar high northern latitudes, 2001-2015*. ORNL DAAC. https://doi.org/10.3334/ORNLDAAC/1526

Mardia, K. V., Kent, J. T., & Bibby, J. M. (1979). *Multivariate analysis*. Academic Press.

Markham, C. (1970). Seasonality of precipitation in the United States. *Annals of the Association of American Geographers*, *60*(3), 593–597. https://doi.org/10.1111/j.1467-8306.1970.tb00743.x

McNally, A., Arsenault, K., Kumar, S., Shukla, S., Peterson, P., Wang, S., et al. (2017). A land data assimilation system for sub-Saharan Africa food and water security applications. *Scientific Data*, *4*(1), 170012. https://doi.org/10.1038/sdata.2017.12

Melchiorre, A., & Boschetti, L. (2018). Global analysis of burned area persistence time with MODIS data. *Remote Sensing*, *10*(5), 750. https://doi.org/10.3390/rs10050750

Midekisa, A., Holl, F., Savory, D. J., Andrade-Pacheco, R., Gething, P. W., Bennett, A., & Sturrock, H. J. W. (2017). Mapping land cover change over continental Africa using Landsat and Google Earth Engine cloud computing. *PLoS One*, *12*(9), e0184926. https://doi.org/10.1371/journal.pone.0184926

Monjarás-Vega, N. A., Briones-Herrera, C. I., Vega-Nieva, D. J., Calleros-Flores, E., Corral-Rivas, J. J., López-Serrano, P. M., et al. (2020). Predicting forest fire kernel density at multiple scales with geographically weighted regression in Mexico. *Science of the Total Environment*, *718*, 137313. https://doi.org/10.1016/j.scitotenv.2020.137313

Mouillot, F., & Field, C. B. (2005). Fire history and the global carbon budget: A 1° × 1° fire history reconstruction for the 20th century. *Global Change Biology*, *11*(3), 398–420. https://doi.org/10.1111/j.1365-2486.2005.00920.X

Mouillot, F., Schultz, M. G., Yue, C., Cadule, P., Tansey, K., Ciais, P., & Chuvieco, E. (2014). Ten years of global burned area products from spaceborne remote sensing—A review: Analysis of user needs and recommendations for future developments. *International Journal of Applied Earth Observation and Geoinformation*, *26*, 64–79. https://doi.org/10.1016/j.jag.2013.05.014

Mulqueeny, C. M., Goodman, P. S., & O'Connor, T. G. (2011). Determinants of inter-annual variation in the area burnt in a semi-arid African savanna. *International Journal of Wildland Fire*, *20*(4), 532–539. https://doi.org/10.1071/wf08141

Murphy, B. P., & Bowman, D. M. J. S. (2007). Seasonal water availability predicts the relative abundance of C_3 and C_4 grasses in Australia. *Global Ecology and Biogeography*, *16*(2), 160–169. https://doi.org/10.1111/j.1466-8238.2006.00285.x

Murphy, B. P., Bradstock, R. A., Boer, M. M., Carter, J., Cary, G. J., Cochrane, M. A., et al. (2013). Fire regimes of Australia: A pyrogeographic model system. *Journal of Biogeography*, *40*(6), 1048–1058. https://doi.org/10.1111/jbi.12065

Murphy, B. P., Williamson, G. J., & Bowman, D. M. J. S. (2011). Fire regimes: Moving from a fuzzy concept to geographic entity. *New Phytologist*, *192*(2), 316–318. https://doi.org/10.1111/j.1469-8137.2011.03893.x

NAFI. (2022). Northern Australian fire information. Retrieved from https://firenorth.org.au/nafi3/

Oliveira, S., Pereira, J. M. C., San Miguel-Ayanz, J., & Lourenco, L. (2014). Exploring the spatial patterns of fire density in Southern Europe using Geographically Weighted Regression. *Applied Geography*, *51*, 143–157. https://doi.org/10.1016/j.apgeog.2014.04.002

Olson, D. M., Dinerstein, E., Wikramanayake, E. D., Burgess, N. D., Powell, G. V. N., Underwood, E. C., et al. (2001). Terrestrial ecoregions of the world: A new map of life on Earth: A new global map of terrestrial ecoregions provides an innovative tool for conserving biodiversity. *BioScience*, *51*(11), 933–938. https://doi.org/10.1641/0006-3568(2001)051[0933:TEOTWA]2.0.CO;2

Pausas, J. G., & Fernández-Muñoz, S. (2012). Fire regime changes in the Western Mediterranean Basin: From fuel-limited to drought-driven fire regime. *Climatic Change*, *110*(1–2), 215–226. https://doi.org/10.1007/s10584-011-0060-6

Pausas, J. G., & Ribeiro, E. (2013). The global fire–productivity relationship. *Global Ecology and Biogeography*, *22*(6), 728–736. https://doi.org/10.1111/geb.12043

Pica-Ciamarra, U., Otte, J., & Chilonda, P. (2007). Livestock policies, land and rural conflicts in sub-Saharan Africa. *Africa*, *07*, 1–20.

Picotte, J. J., Bhattarai, K., Howard, D., Lecker, J., Epting, J., Quayle, B., et al. (2020). Changes to the Monitoring Trends in Burn Severity program mapping production procedures and data products. *Fire Ecology*, *16*(1), 1–12. https://doi.org/10.1186/s42408-020-00076-y

Ramo, R., Roteta, E., Bistinas, I., van Wees, D., Bastarrika, A., Chuvieco, E., & van der Werf, G. R. (2021). African burned area and fire carbon emissions are strongly impacted by small fires undetected by coarse resolution satellite data. *Proceedings of the National Academy of Sciences*, *118*(9), e2011160118. https://doi.org/10.1073/pnas.2011160118

R Core Team. (2017). *R language definition*. R Foundation for Statistical Computing.

Rienecker, M. M., Suarez, M. J., Gelaro, R., Todling, R., Bacmeister, J., Liu, E., et al. (2011). MERRA: NASA's Modern-Era retrospective analysis for research and applications. *Journal of Climate*, *24*(14), 3624–3648. https://doi.org/10.1175/JCLI-D-11-00015.1

Rosenzweig, M. L. (1968). Net primary productivity of terrestrial communities: Prediction from climatological data. *The American Naturalist*, *102*(923), 67–74. https://doi.org/10.1086/282523

Roy, D. P., Huang, H., Boschetti, L., Giglio, L., Yan, L., Zhang, H. H., & Li, Z. (2019). Landsat-8 and Sentinel-2 burned area mapping - A combined sensor multi-temporal change detection approach. *Remote Sensing of Environment*, *231*, 0034–4257. https://doi.org/10.1016/j.rse.2019.111254

Russell-Smith, J., Yates, C. P., Whitehead, P. J., Smith, R., Craig, R., Allan, G. E., et al. (2007). Bushfires' down under': Patterns and implications of contemporary Australian landscape burning. *International Journal of Wildland Fire*, *16*(4), 361–377. https://doi.org/10.1071/WF07018

Saha, M. V., Scanlon, T. M., & D'Odorico, P. (2019). Climate seasonality as an essential predictor of global fire activity. *Global Ecology and Biogeography*, *28*(2), 198–210. https://doi.org/10.1111/geb.12836

Sanderson, E. W., Jaiteh, M., Levy, M. A., Redford, K. H., Wannebo, A. V., & Woolmer, G. (2002). The Human Footprint and the Last of the Wild the human footprint is a global map of human influence on the land surface, which suggests that human beings are stewards of nature, whether we like it or not. *BioScience*, *52*(10), 891–904. https://doi.org/10.1641/0006-3568(2002)052[0891:THFATL]2.0.CO;2

Sankaran, M., Hanan, N. P., Scholes, R. J., Ratnam, J., Augustine, D. J., Cade, B. S., et al. (2005). Determinants of woody cover in African savannas. *Nature*, *438*(7069), 846–849. https://doi.org/10.1038/nature04070

San-Miguel-Ayanz, J., Schulte, E., Schmuck, G., Camia, A., Strobl, P., Liberta, G., et al. (2012). Comprehensive monitoring of wildfires in Europe: The European forest fire information system (EFFIS). In *Approaches to managing disaster - assessing Hazards, emergencies and disaster impacts*. https://doi.org/10.5772/28441

21698961, 2022, 8, Downloaded from https://agupubs.onlinelibrary.wiley.com/doi/10.1029/2021JG006694 by University Of Maryland, Wiley Online Library on [27/09/2023]. See the Terms and Conditions (https://onlinelibrary.wiley.com/terms-and-conditions) on Wiley Online Library for rules of use; OA articles are governed by the applicable Creative Commons License

Staver, A. C., Archibald, S., & Levin, S. A. (2011). The global extent and determinants of savanna and forest as alternative biome states. *Science*, *334*(6053), 230–232. https://doi.org/10.1126/science.1210465

Stevens, N., Lehmann, C. E. R., Murphy, B. P., & Durigan, G. (2017). Savanna woody encroachment is widespread across three continents. *Global Change Biology*, *23*(1), 235–244. https://doi.org/10.1111/gcb.13409

Syphard, A. D., Keeley, J. E., Pfaff, A. H., & Ferschweiler, K. (2017). Human presence diminishes the importance of climate in driving fire activity across the United States. *Proceedings of the National Academy of Sciences*, *114*(52), 13750–13755. https://doi.org/10.1073/pnas.1713885114

Toté, C., Patricio, D., Boogaard, H., van der Wijngaart, R., Tarnavsky, E., & Funk, C. (2015). Evaluation of satellite rainfall estimates for drought and flood monitoring in Mozambique. *Remote Sensing*, *7*(2), 1758–1776. https://doi.org/10.3390/rs70201758

van Langevelde, F., Van De Vijver, C. A. D. M., Kumar, L., Van De Koppel, J., De Ridder, N., Van Andel, J., et al. (2003). Effects of fire and herbivory on the stability of savanna ecosystems. *Ecology*, *84*(2), 337–350. https://doi.org/10.1890/0012-9658(2003)084[0337:eofaho]2.0.co;2

van der Werf, G. R., Randerson, J. T., Giglio, L., Gobron, N., & Dolman, A. J. (2008). Climate controls on the variability of fires in the tropics and subtropics. *Global Biogeochemical Cycles*, *22*(3), GB3028. https://doi.org/10.1029/2007GB003122

van der Werf, G. R., Randerson, J. T., Giglio, L., van Leeuwen, T. T., Chen, Y., Rogers, B. M., et al. (2017). Global fire emissions estimates during 1997–2016. *Earth System Science Data*, *9*(2), 697–720. https://doi.org/10.5194/essd-9-697-2017

Ward, J. H., Jr. (1963). Hierarchical grouping to optimize an objective function. *Journal of the American Statistical Association*, *58*(301), 236–244. https://doi.org/10.1080/01621459.1963.10500845

Whitman, E., Batllori, E., Parisien, M.-A., Miller, C., Coop, J. D., Krawchuk, M. A., et al. (2015). The climate space of fire regimes in north-western North America. *Journal of Biogeography*, *42*(9), 1736–1749. https://doi.org/10.1111/jbi.12533

Wilcoxon, F. (1945). Individual comparisons by ranking methods. *Biometric Bulletin*, *1*(6), 80–83. https://doi.org/10.2307/3001968

Wilks, D. (2005). *Statistical methods in the atmospheric sciences*. Academic Press.

Willmott, C. J., Rowe, C. M., & Mintz, Y. (1985). Climatology of the terrestrial seasonal water cycle. *Journal of Climatology*, *5*(6), 589–606. https://doi.org/10.1002/joc.3370050602

Wood, S., & Wood, M. S. (2017). *Package 'mgcv'* (Vol. 1–7). R Package Version.

Yang, Y., Long, D., & Shang, S. (2013). Remote estimation of terrestrial evapotranspiration without using meteorological data. *Geophysical Research Letters*, *40*(12), 3026–3030. https://doi.org/10.1002/grl.50450

Zubkova, M., Boschetti, L., Abatzoglou, J. T., & Giglio, L. (2019). Changes in fire activity in Africa from 2002 to 2016 and their potential drivers. *Geophysical Research Letters*, *46*(13), 7643–7653. https://doi.org/10.1029/2019GL083469

21698961, 2022, 8, Downloaded from https://agupubs.onlinelibrary.wiley.com/doi/10.1029/2021JG006694 by University Of Maryland, Wiley Online Library on [27/09/2023]. See the Terms and Conditions (https://onlinelibrary.wiley.com/terms-and-conditions) on Wiley Online Library for rules of use; OA articles are governed by the applicable Creative Commons License